AFGL-TR-80-0066
ENVIRONMENTAL RESEARCH PAPERS, NO. 696

Hemispheric Asymmetries Detected From Satellite Ionization Gauge Measurements

JOSEPH P. McISAAC

25 February 1980

AERONOMY DIVISION PROJECT 6690
AIR FORCE GEOPHYSICS LABORATORY
HANSCOM AFB, MASSACHUSETTS 01731

AIR FORCE SYSTEMS COMMAND, USAF

This report has been reviewed by the ESD Information Office (OI) and is releasable to the National Technical Information Service (NTIS).

This technical report has been reviewed and is approved for publication.

FOR THE COMMANDER

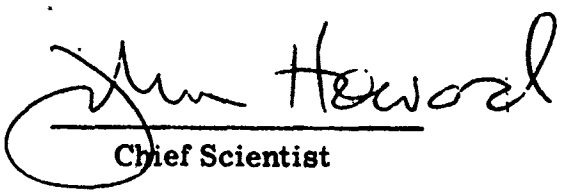

Chief Scientist

Qualified requestors may obtain additional copies from the Defense Documentation Center. All others should apply to the National Technical Information Service.

(9) ENVIRONMENTAL RESEARCH PAPERS,

Unclassified

SECURITY CLASSIFICATION OF THIS PAGE (When Data Entered)

REPORT DOCUMENTATION PAGE	READ INSTRUCTIONS BEFORE COMPLETING FORM
(14) 1. REPORT NUMBER AFGL-TR-80-0066 AFGL-ERP-696	2. GOVT ACCESSION NO ADA090339	3. RECIPIENT'S CATALOG NUMBER
(5) 4. TITLE (and Subtitle) HEMISPHERIC ASYMMETRIES DETECTED FROM SATELLITE IONIZATION GAUGE MEASUREMENTS	5. TYPE OF REPORT & PERIOD COVERED Scientific. Interim,
	6. PERFORMING ORG. REPORT NUMBER ERP No. 696
(10) 7. AUTHOR(s) Joseph P. McIsaac	8. CONTRACT OR GRANT NUMBER(s) (16) 6690 (17) 01
9. PERFORMING ORGANIZATION NAME AND ADDRESS Air Force Geophysics Laboratory (LKB) Hanscom AFB Massachusetts 01731	10. PROGRAM ELEMENT, PROJECT, TASK AREA & WORK UNIT NUMBERS 62101F 66900707
11. CONTROLLING OFFICE NAME AND ADDRESS Air Force Geophysics Laboratory (LKB) Hanscom AFB Massachusetts 01731	12. REPORT DATE (11) 25 February 1980
	13. NUMBER OF PAGES (12) 49
14. MONITORING AGENCY NAME & ADDRESS(if different from Controlling Office)	15. SECURITY CLASS. (of this report) Unclassified
	15a. DECLASSIFICATION/DOWNGRADING SCHEDULE

16. DISTRIBUTION STATEMENT (of this Report)

Approved for public release; distribution unlimited.

17. DISTRIBUTION STATEMENT (of the abstract entered in Block 20, if different from Report)

18. SUPPLEMENTARY NOTES

19. KEY WORDS (Continue on reverse side if necessary and identify by block number)

Neutral density
Thermosphere
Direct measurements
Tidal effects
Hemispheric asymmetries

20. ABSTRACT (Continue on reverse side if necessary and identify by block number)

Results obtained from the S3-1 ionization gauge measurements are statistically examined for hemispheric asymmetries in neutral density behavior. The parameter analyzed in this study is the mean value $\overline{R}$, the ratio of the measured density to the Jacchia 71 model value. Over 150,000 values obtained during the period from November 1974 to May 1975 and covering the altitude range from perigee (about 160 km) to 300 km are considered. Results are presented in the form of frequency histograms and graphs of mean ratios vs latitude. Significant hemispherical asymmetries are found and described in detail.

DD FORM 1 JAN 73 1473

Unclassified

SECURITY CLASSIFICATION OF THIS PAGE (When Data Entered)

409 512

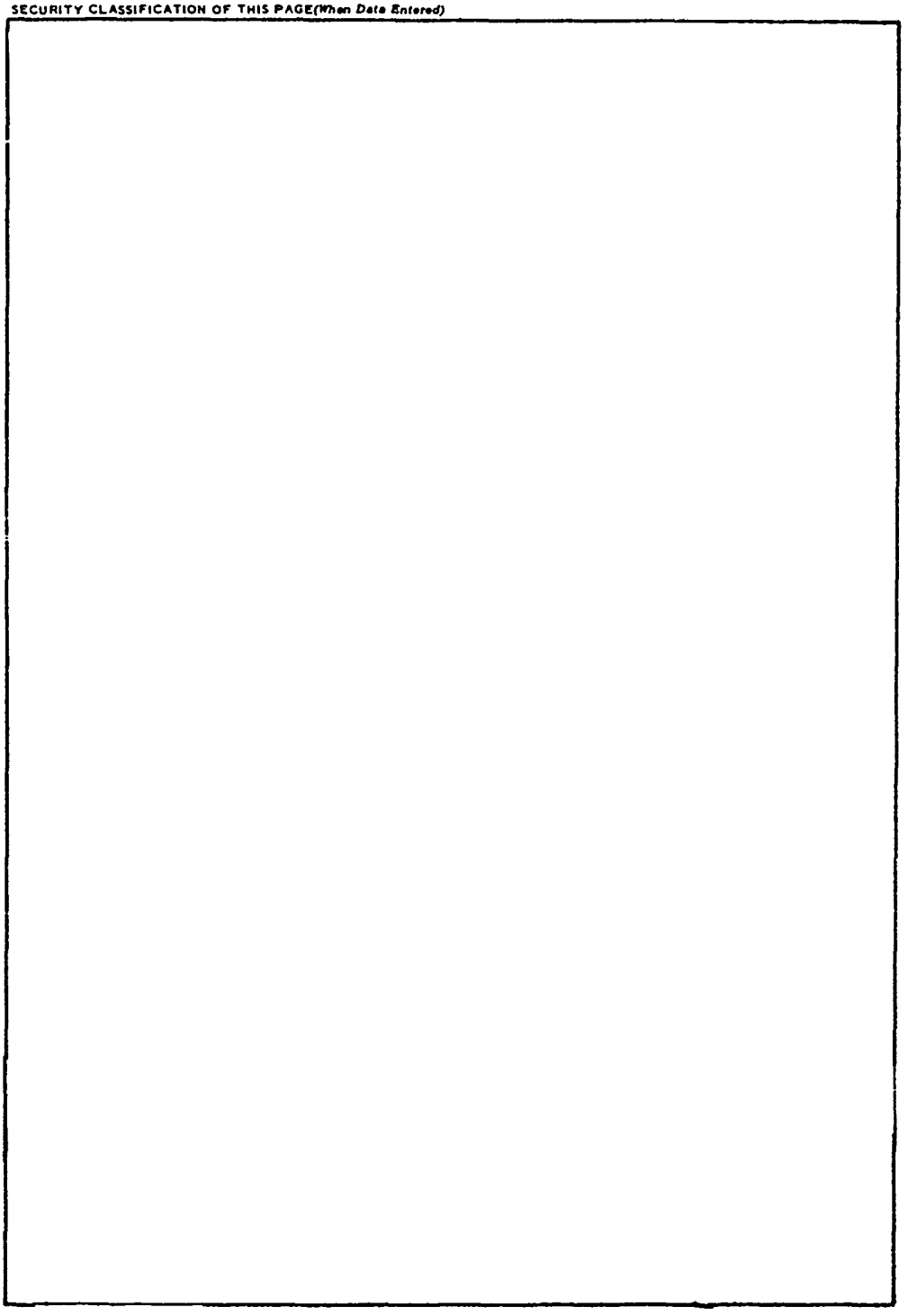

Preface

The author is indebted to Dennis Delorey of Boston College's Space Data Analysis Laboratory for computer programming and plotting routines. This work was performed under Contract No. F19628-76-C-0190 with the Analysis and Simulation Branch of the Air Force Geophysics Laboratory.

Contents

Illustrations

Illustrations

Tables

Hemispheric Asymmetries Detected From Satellite Ionization Gauge Measurements

1. INTRODUCTION

The ionization gauge experiment successfully flown onboard the Air Force S3-1 satellite resulted in the accumulation of an extensive file of neutral density measurements taken over the period extending from November 1974 to May 1975. This report is a first attempt at performing an analysis of the total data file gathered as a result of the S3-1 flight. The satellite orbit, experiment details, reduction procedures including computer flow charts, and representative results have been previously presented and described in detail in earlier reports.[1,2] The statistical analysis performed here is similar to that done by Forbes et al[3] in which the statistical parameter analyzed is the ratio R between the measured density and a model density. Frequency distribution plots of R together with mean values and standard deviations are given for different levels of geomagnetic activity. The three levels of geomagnetic activity used are characterized as quiet, moderate, and

(Received for publication 22 February 1980)

1. McIsaac, J.P., Champion, K.S.W., McInerney, R.E., and Delorey, D. (1976) Ionization Gauge Measurements of Atmospheric Density From a Low Altitude Satellite, AFGL-TR-76-0113, AD A032373.

2. McIsaac, J.P., McInerney, R.E., and Delorey, D. (1978) Satellite Ionization Gauge Measurements of Atmospheric Density, AFGL-TR-78-0201, AD A061613.

3. Forbes, J.M., Marcos, F.A., and Gillette, D.F. (1979) An Evaluation of Thermospheric Models, AFGL-TR-79-0140, AD B036638.

disturbed levels. Comparisons of north and south hemispheric ratios are constructed over a range of different altitudes and latitudes for the levels of geomagnetic activity given above. The ratio analysis provides a more meaningful comparison of the relative hemispheric behavior of atmospheric density than would a comparison of the density measurements alone. This is so because the S3-1 satellite measurements were obtained over relatively short spatial intervals, that is, the satellite's data acquisition duty cycle routinely involved the taking of one perigee pass every alternate revolution. A perigee pass consisted of a 20-min tape recording centered around the time of perigee occurrance. The net result was a very large accumulation of measurements under diverse conditions of local time, latitude, longitude, altitude, season, and varied geophysical conditions of solar flux and geomagnetic activity. Figure 1 provides a time history of the satellite's perigee locations in terms of altitude, local time, and latitude. In this report the Jacchia 1971 model[4] is used to form the ratio parameters, where the model values are adjusted to the appropriate conditions pertaining to the time of each measurement. An advantage in using the J71 model for forming the ratio parameter is that the latitudinal variation of the diurnal bulge in the Jacchia model is symmetrical in both hemispheres wherein the maximum density migrates north and south of the equator in phase with the sub-solar point. A disadvantage to the use of any model in determining the ratio parameter is that whatever model is employed, inherent in the ratios are the inadequacies of the modelling technique as well as unmodelled real atmospheric differences.

2. STATISTICAL PROCEDURE

The three parameters derived from the data base are the mean ratio $\overline{R}$ (mean of the ratios, data/J71), the standard deviation σ_R and N the total number of measurements. The expressions used to determine $\overline{R}$ and σ_R are as follows:

$$\overline{R} = \frac{1}{N} \sum_{m=1}^{N} R_m \tag{1}$$

and

$$\sigma_R = \left[\frac{1}{N-1} \sum_{m=1}^{N} (R_m - \overline{R})^2 \right]^{1/2} \tag{2}$$

4. Jacchia, L.G. (1971) Revised Static Models of the Thermosphere and Exosphere With Empirical Temperature Profiles, Spec. Rpt. 332, Smithsonion Astrophys. Observatory, Cambridge, MA.

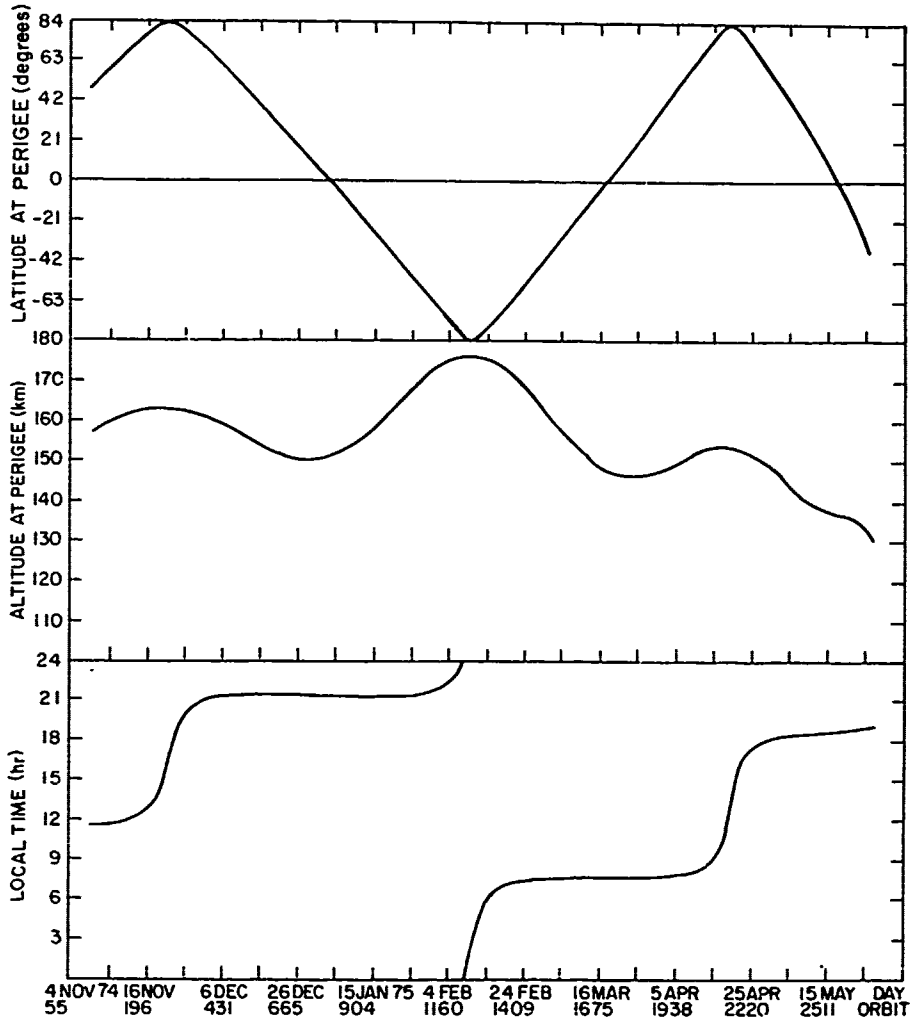

Figure 1. Satellite Position in Terms of Perigee Location, With Local Time, Altitude and Latitude of Perigee Given as a Function of Date and Orbit Number

The data base is divided into different combinations of parameters to form data sets. Within each set, the total number of points (ratios) are sorted in terms of their occurrence and partitioned into fixed intervals to form frequency histograms. For each histogram the three parameters $\overline{R}$, σ_R and N are computed and a normal distribution curve constructed which is then superimposed over the histogram. The expression used in deriving the normal distribution curve[5] is:

5. Freeman, H. (1963) Introduction to Statistical Inference, p 140, Addison-Wesley Publishing Co.

$$Y = \frac{i\,N}{\sigma_R \sqrt{2\pi}}\; e^{\frac{-(R-\bar{R})^2}{2\sigma_R^2}} \qquad (3)$$

where Y, the ordinate, is the number of occurrences per interval i. The normal curve superimposition although interesting is not too significant. Its worth is greatest when used for model evaluations. Some insight, however, is gained from histogram examination as one can determine how results are distributed about their means and detect asymmetric distributions. The real value of the statistical treatment is derived from the employment of the mean ratios and the variation of these ratios under diverse combinations of solar, geophysical and global conditions obtainable from an extensive data base. Used in this manner the statistical analysis provides an excellent technique for investigating average atmospheric behavior and examining systematic variations.

3. DATA

The data base partitioning used in this report is shown in Figure 2 and the respective sample size for each bin category is shown in Figure 3. As seen in Figure 2, the base is first separated into the two central divisions of northern and southern hemispheric data followed by a further division into three sub-levels. The first sub-level separates hemispheric data according to the degree of geomagnetic activity; quiet, moderate, or disturbed. Or more precisely, the geomagnetic division is determined by the value of the K_p planetary index (6 hr lag). The range limits for the activity levels used are:

Quiet activity (low): $0 \leq K_p \leq 3$

Moderate activity (moderate): $3 < K_p \leq 5$

Disturbed activity (high): $5 < K_p \leq 9$.

The second and third sub-level breakdowns are by altitude and latitude respectively. These breakdowns are determined in a straightforward manner reflecting a compromise between adequate statistical sample sizes and a desire to avoid an excessive number of computer runs needed to compute numerical values and to run off plotting routines. The partitioning as given in Figure 2 involved the generation of 135 frequency histograms, a portion of which are shown in the appendix. In addition to the above, various bins were combined to provide larger bins resulting in more histogram computations. An example of this is shown in Table 1 where combinations of several bins were constructed in order to develop a more meaningful comparison between gauge results shown here and those obtained from another technique.

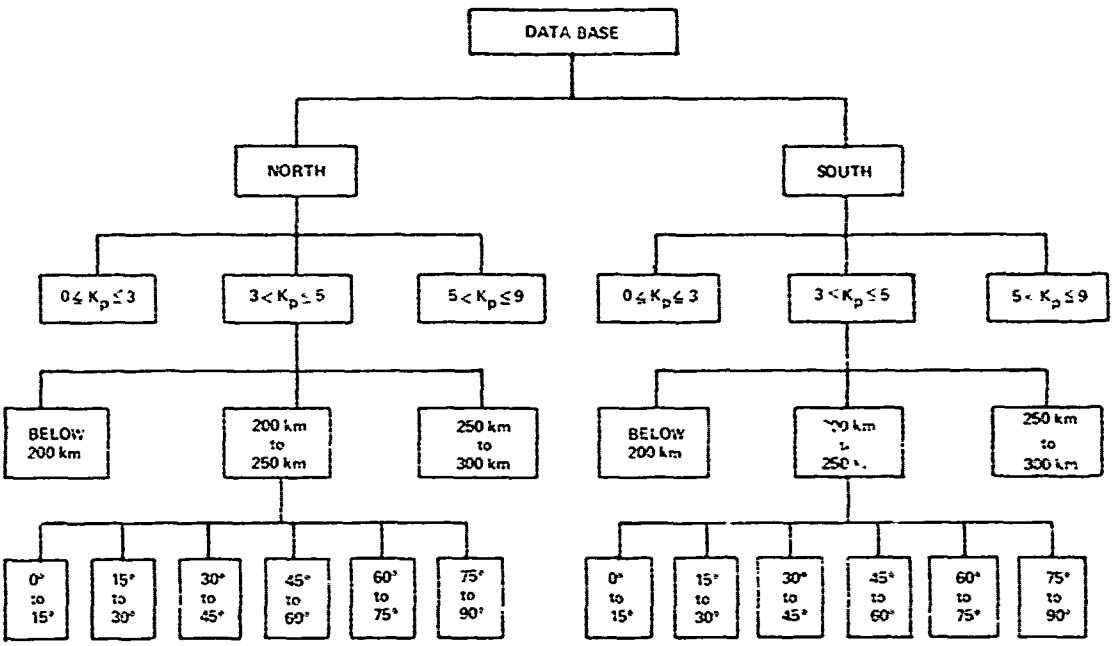

Figure 2. Partition Diagram Outlining Data Base Division

Histograms with normal curves superimposed are included in the appendix together with legend data consisting of values of $\overline{R}$, σ_R, N and the normalized Y value as well as the parameters that define the bin confines. Only a portion of the total number of histograms generated as a result of the bin partitioning has been included in the appendix. However, that portion is representative of the full histogram set. Figures, which are discussed in detail in the following section, representing mean behavior of neutral density over the globe, were developed that show results as a function of altitude under different conditions of geomagnetic activity and over several altitude regions.

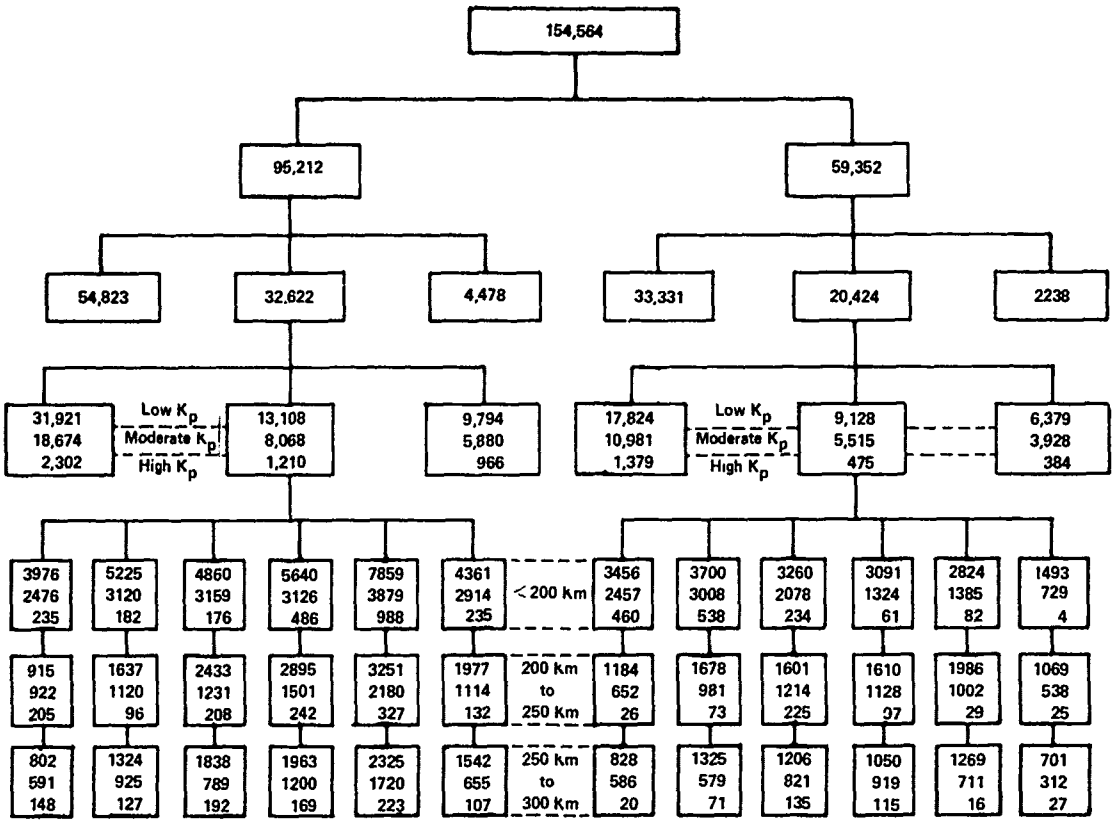

Figure 3. Sample Sizes Resulting From Data Base Partition Given in Figure 2.

4. DISCUSSION

Figure 4 shows differences between mean ratios at corresponding latitudes in the north and south hemispheres plotted as a function of latitude. The ratio differences are given for three levels of geomagnetic conditions; quiet, moderate, and disturbed, and for three altitude regions. Among the prominent features seen in this set of curves, perhaps most outstanding is the total absence of positive differences below 200 km over all latitudes. Only at higher altitudes and in regions about the equator do we observe positive ratio differences. The shapes of the difference curves above 200 km, also appear to develop into similar basic patterns that tend to be accentuated as the level of geomagnetic increases. This structural pattern is manifested in greater detail in the later figures.

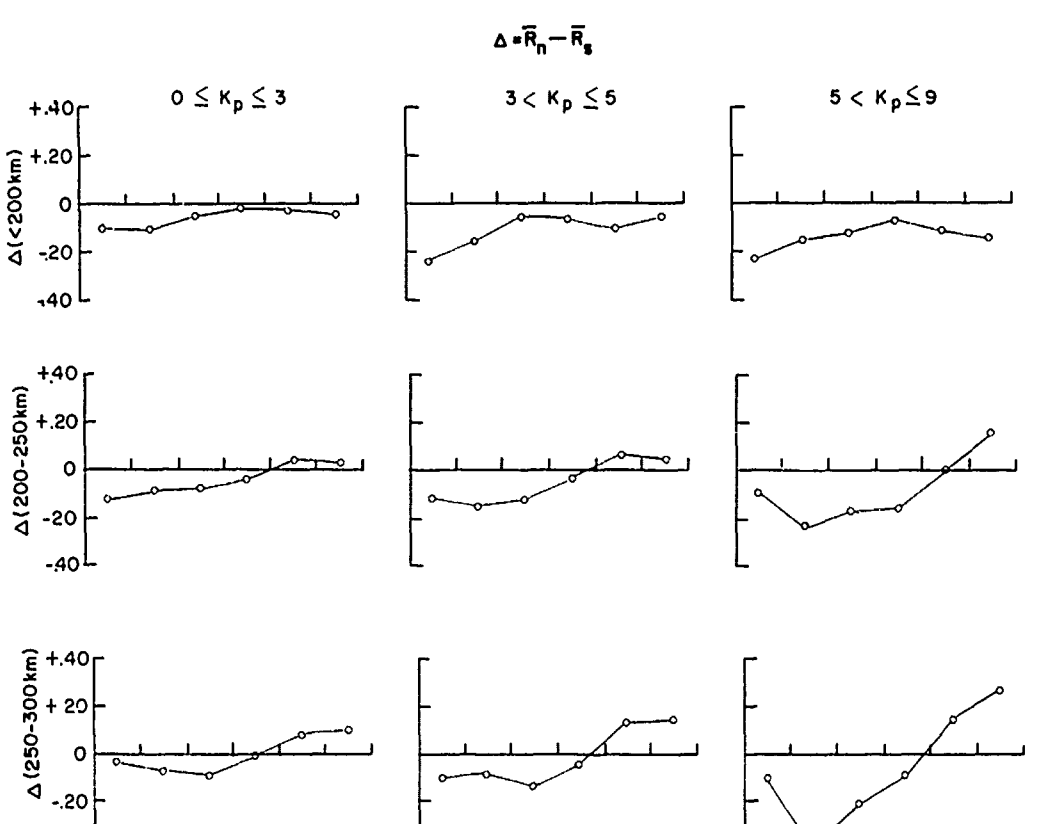

Figure 4. Differences in Average Density Ratio vs Latitude for Three Geomagnetic Groups. Top left to right: low, moderate and high activity. Top for altitudes less than 200 km, middle for altitudes 200 to 250 km and bottom for altitudes 250 to 300 km

The overall negative differences seen in Figure 4 indicate that atmospheric density over the period of this study was greater over the southern hemisphere, which is in agreement with what was found by Barlier et al.[6,7] His examination of over 12,000 values obtained from drag data of satellites indicated that densities in the southern hemisphere were systematically larger than or equal to the corresponding values in the northern hemisphere. However, in terms of atomic oxygen

6. Barlier, F., Perret, D., and Jaeck, C. (1973) Structure of the neutral atmosphere between 150 and 500 km, Space Research XIII:349-355.

7. Barlier, F., Bauer, P., Jaeck, C., Thuillier, G., and Kockharts, G. (1974) North-south asymmetries in the thermosphere during the last maximum of the solar cycle, J. Geophys. Res. 79:5273-5285.

concentrations, it[7] was shown that at 200 km the concentrations tended to accumulate over the cold hemisphere (winter) at the lower latitudes where seasonal effects did not dominate, which also is not in disagreement with what we observe in Figure 4.

It is interesting to note that the Jacchia 71 model treats hemispheric variations in a uniform manner, that is, the diurnal maximum migrates symmetrically about the equator in phase with the declination angle. In forming our ratios the normalization of the density measurement to the J71 model value should, in practice, compensate somewhat for the seasonal effects due to the migration of the diurnal bulge across the equator. As the southern hemisphere measurements in our data base were taken almost entirely during the summer season, the appropriate southern hemispheric J71 model values will, all other factors being equal, be greater than the J71 northern hemispheric values (spring/fall); consequently, from the model viewpoint the north hemispheric ratios should be larger than south hemispheric ratios.

Figure 5 illustrates global latitudinal structure more clearly; shown here are ratios of measured densities to model densities given as a function of north and south latitudes for three altitude regions and different levels of geomagnetic activity. In the low altitude (< 200 km) curve set, northern ratios are fairly constant while southern ratios increase in the direction of the pole. Again, southern ratios are seen to be considerably larger than northern ratios. There appears to be little noticeable effect from increasing geomagnetic activity at the lower altitudes. For the higher altitude curve sets, two prominent features stand out; the enhancement in the southern auroral region during periods when $K_p > 5$ and the north-south bulge/trough structure located about the equator. It is also interesting to note that for the most part the ratio magnitudes appear to be inversely proportional to the level of geomagnetic activity indicating the J71 model overcompensates for geomagnetic effects. The auroral region enhancement is present only in the southern hemisphere auroral region where, unlike the data below 200 km, the density is seen to decrease poleward of the auroral region. This same effect was observed by Forbes et al[8] from accelerometer data taken onboard the NASA AE-C satellite, however, in that report north and south latitudes were not separated. This particular feature found here and in the AE-C results was deduced in both cases from rather small statistical data samples, therefore the observations regarding the auroral region feature; enhancement and subsequent poleward drop-off, should be viewed as inconclusive. Rice and Sharp[9] have reported observations

8. Forbes, J.M., Marcos, F.A., and Champion, K.S.W. (1977) Lower thermosphere response to geomagnetic activity, Space Res. XVIII:173-176.

9. Rice, C.J., and Sharp, L.R. (1977) Neutral Atmospheric Waves in the Thermosphere and Tropospheric Weather System, SAMSO-TR-77-98.

from the ion gauge measurements performed onboard the AE-C spacecraft wherein they observed an asymmetric auroral region feature consisting of a southern latitude region (40° to 68°S) in which there was a high occurrence of wavelike structural features not seen in the corresponding northern latitude region.

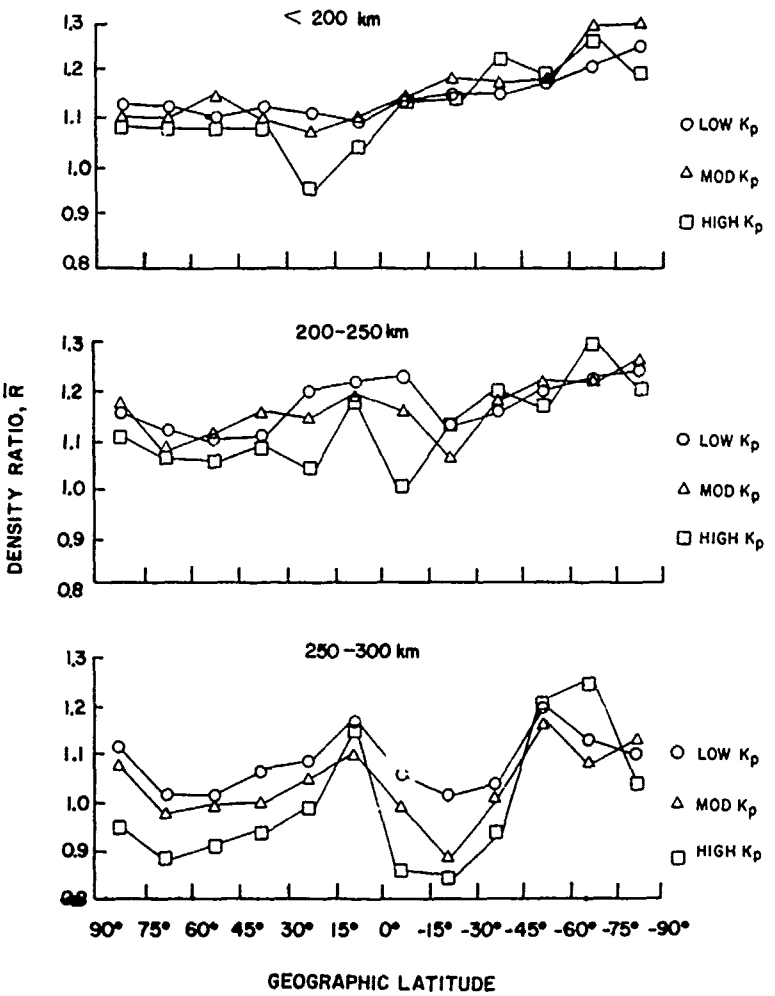

Figure 5. Average Density Ratio vs Geographic Latitude for Three Altitude Regions < 200 km, 200 to 250 km, and 250 to 300 km. Open circles are low K_p values, triangles are for moderate K_p values and squares are for high K_p values

The other prominent structure observation apparent in Figure 5 is the equatorial asymmetry, a north-south, bulge/trough formation located about the equator. This bulge/trough equatorial feature is highly visible at the higher altitudes but seems to disappear below 200 km. Certain aspects or characteristics of this structure are more evident in Figure 6 where ratio curves are grouped together in sets according to the level of geomagnetic activity. Foremost, is the phase relationship between ratios below 200 km to those above 200 km. The equatorial structure below 200 km is clearly out of phase with the structure above 200 km. Below 200 km at northern equatorial latitudes there is a trough in place of the bulge seen at altitudes above 200 km. In a like manner, the deep southern latitude trough at high altitudes is reversed at low altitudes and although one does not observe a well defined bulge at the southern latitudes below 200 km, one can observe a shape that suggests a bulge merged with other effects. A second characteristic of the equatorial structure apparent in both Figures 5 and 6 is that the minimum of the southern latitude trough appears to drift towards the equator during periods of increase geomagnetic activity ($K_p > 5$).

Equatorial located structure of a similar nature has been reported elsewhere[10, 11] and, although no explanations were given by the authors, in each case the structure was characterized as persistent as opposed to being of a transient nature. The persistent nature of the structure described here requires a non-transient type mechanism be invoked if a satisfactory explanation is to be found. Recall that the ratio values are mean values representative of data obtained over a six month period. One possible explanation would involve solar tidal variations of density. The north-scuth pattern observed in our data set is suggestive of tidal mode propagation into the thermosphere with antisymmetric, semidiurnal modes dominant. Semidiurnal tidal effects have been theoretically examined by Hong and Lindzen[12] and large equatorial latitudinal variations, particularly at solar cycle minimum, have been predicted. Our data base lacks adequate local time coverage to properly evaluate tidal oscillations as an explanation. However, although not shown in this report, the data given in Figures 5 and 6 have been further constrained to periods of constant local time (± 1 hr). The two local time periods were at 0700 and 2200 hours. Under this added constraint of constant local time the observed structural features remained basically unchanged indicating that the variations in the data are not due to differences in local time.

---

10. Philbrick, C. R., and McIsaac, J. P. (1972) Measurements of atmospheric composition near 400 km, Space Research XVI:743-749.

11. Ching, B. K., and Carter, V. L. (1974) Ion gauge measurements of latitudinal density variations at night, Geophys. Res. Lett. 1:93-96.

12. Hong, S. S., and Lindzen, R. S. (1976) Solar semidiurnal tide in the thermosphere, J. Atmos. Sci. 33:135-153.

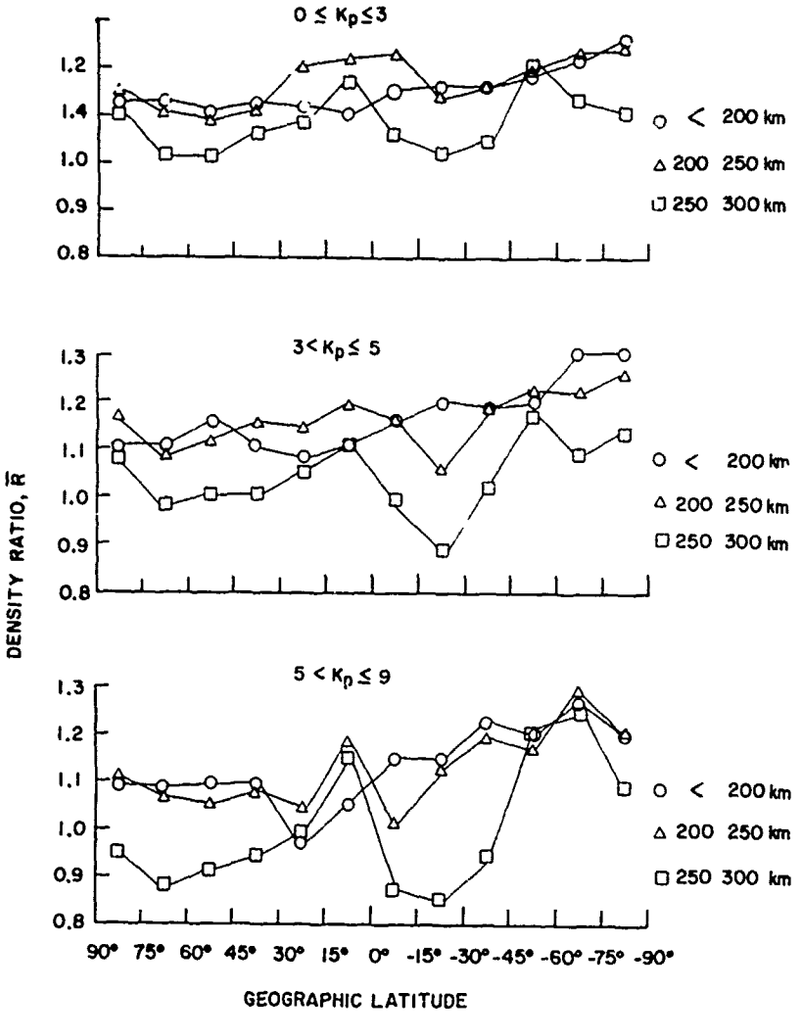

Figure 6. Average Density Ratio vs Latitude for Three Levels of Geomagnetic Activity as Shown. Altitude symbols are circles < 200 km, triangles 200 to 250 km and squares 250 to 300 km

A point that requires investigation is the absence of the structural features discussed above from the accelerometer results[13] obtained onboard the same S3-1 spacecraft. In an attempt to ascertain the reason for this discrepancy the gauge ratio parameters given in this report were recomputed to coincide with the

13. Marcos, F.A., McInerney, R.E., and Fioretti, R.W. (1978) Variability of the Lower Thermosphere Determined From Satellite Accelerometer Data, AFGL-TR-78-0134, AD A058-982.

partitioning used by Marcos et al in their processing of accelerometer results. This new partitioning of the gauge data involved combining the two altitude bins of < 200 km and 200 to 250 km to form a single bin extending from perigee to 250 km and expanding the latitude spans by 15° to form 30° bins. Putting results from both techniques in the same format provides a means for directly comparing results. This is done in Table 1 where results from both data sets are listed. Also, the data shown in Table 1 are plotted as a function of latitude (Figure 7). Referring to Figure 7, one readily observes that the figure shows two pairs of curves for two levels of geomagnetic activity in which results from each technique are compared. The upper and lower curve sets can be referred to as representing high and low geomagnetic, respectively, although the K_p limits for both sets are slightly different. Marcos et al[13] omitted data in the K_p range from $2.6 \leqq K_p \leqq 3.6$ in order to emphasize the differences between the high and low K_p data groups. Also, in that study, there was no separate geomagnetic activity category that could be characterized as moderate, hence, a comparison of results for moderate geomagnetic conditions is omitted. Upon examination of Figure 7 one can observe that the agreement between results obtained from both techniques is generally good, particularly in the equatorial region where the structure reported in this report has been observed. The region of greatest discrepancy is in the high southern latitudes which is also the region where statistics are poorest. Accelerometer results also indicate higher southern hemispheric densities. One fact made immediately evident from Figure 7 is that when the ionization gauge results are configured in the format used in the accelerometer study, the results reveal little of the structure reported here; hence, indicating no general disagreement between the two techniques. Two reasons are offered for the lack of structure seen in Figure 7, namely, the bin limits were too broad (latitude and altitude) and, certainly a major factor, the altitude dependent phase reversal behavior reported here. By grouping data from below 200 km with data above 200 km, the result is a tendency to smear or negate the structural differences between the two altitude regions.

Table 1. Comparison of Accelerometer and Ionization Gauge Results Obtained Onboard the S3-1 Satellite

Ionization Gauge Results				Accelerometer Results			
Latitude Range	K_p Range	Number of Points	Mean Value	Latitude Range	K_p Range	Number of Points	Mean
90°N - 60°N	$0 \leq K_p \leq 3$	17,448	1.13	90°N - 60°N	$0 \leq K_p \leq 2.6$	3697	1.05
60°N - 30°N	$0 \leq K_p \leq 3$	15,828	1.12	60°N - 30°N	$0 \leq K_p \leq 2.6$	2177	1.02
30°N - 0°	$0 \leq K_p \leq 3$	11,753	1.13	30°N - 0°	$0 \leq K_p \leq 2.6$	1204	1.11
0° - 30°S	$0 \leq K_p \leq 3$	10,018	1.15	0° - 30°S	$0 \leq K_p \leq 2.6$	1529	1.14
30°S - 60°S	$0 \leq K_p \leq 3$	9,562	1.17	30°S - 60°S	$0 \leq K_p \leq 2.6$	1717	1.09
60°S - 90°S	$0 \leq K_p \leq 3$	7,372	1.23	60°S - 90°S	$0 \leq K_p \leq 2.6$	988	1.05
90°N - 60°N	$5 < K_p \leq 9$	1682	1.09	90°N - 60°N	$4 < K_p \leq 9$	2163	1.03
60°N - 30°N	$5 < K_p \leq 9$	1112	1.08	60°N - 30°N	$4 \leq K_p \leq 9$	1945	1.02
30°N - 0°	$5 < K_p \leq 9$	718	1.08	30°N - 0°	$4 \leq K_p \leq 9$	1424	1.07
0° - 30°S	$5 < K_p \leq 9$	1097	1.15	0° - 30°S	$4 < K_p \leq 9$	1180	1.10
30°S - 60°S	$5 < K_p \leq 9$	617	1.20	30°S - 60°S	$4 \leq K_p \leq 9$	1165	1.05
60°S - 90°S	$5 < K_p \leq 9$	140	1.25	60°S - 90°S	$4 \leq K_p \leq 9$	396	1.11

Altitude range is from 250 km to perigee.

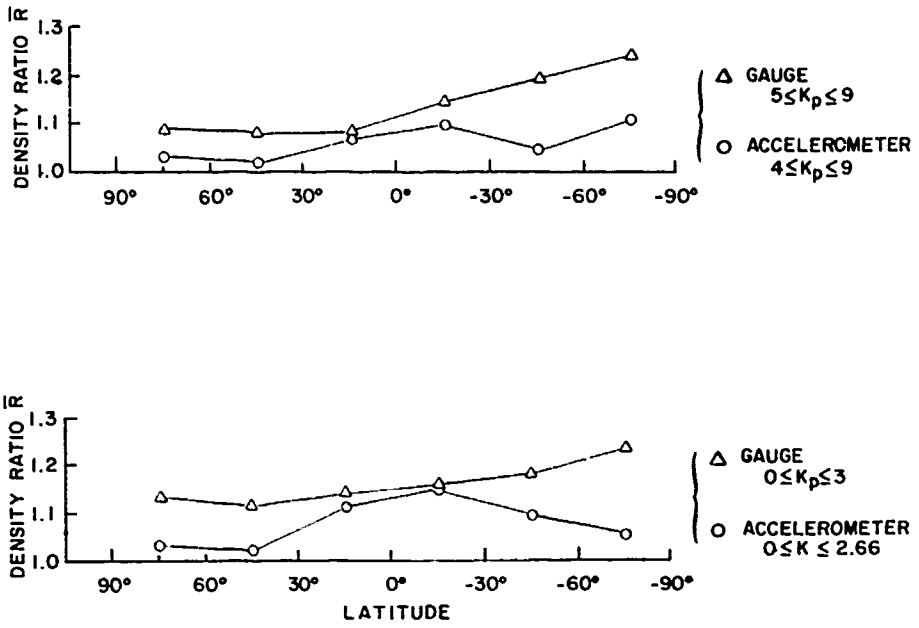

Figure 7. Ratios vs Latitude for Two S3-1 Satellite Experiments. Triangles are ionization gauge values, circles are accelerometer values

5. SUMMARY AND CONCLUSION

A statistical analysis of thermospheric density measurements, in excess of 150,000 values, described in this report has revealed hemispheric asymmetries. In general, at least for the period of this study, southern hemispheric densities are found to be greater relative to the Jacchia 71 model than northern hemisphere densities. Density enhancements are observed in the southern auroral region under disturbed geomagnetic conditions ($K_p > 5$) that are not seen in the corresponding north auroral region. A non-transient, equatorial-located, structural feature is observed. This structure which is asymmetric about the equator, is seen to intensify with increasing altitude and geomagnetic activity. A tentative explanation is advanced that attributes the equatorial behavior to atmospheric tidal effects. Further analysis of these results is planned to investigate seasonal influence upon the observed equatorial structure and determine the fine spatial resolution, as well.

References

1. McIsaac, J.P., Champion, K.S.W., McInerney, R.E., and Delorey, D. (1976) Ionization Gauge Measurements of Atmospheric Density From a Low Altitude Satellite, AFGL-TR-76-0113, AD A032373.
2. McIsaac, J.P., McInerney, R.E., and Delorey, D. (1978) Satellite Ionization Gauge Measurements of Atmospheric Density, AFGL-TR-78-0201, AD A061613.
3. Forbes, J.M., Marcos, F.A., and Gillette, D.F. (1979) An Evaluation of Thermospheric Models, AFGL-TR-79-0140, AD B36638.
4. Jacchia, L.G. (1971) Revised Static Models of the Thermosphere and Exosphere With Empirical Temperature Profiles, Spec. Rpt. 332, Smithsonian Astrophys. Observatory, Cambridge, MA.
5. Freeman, H. (1963) Introduction to Statistical Inference, p 140, Addison-Wesley Publishing Co.
6. Barlier, F., Perret, D., and Jaeck, C. (1973) Structure of the neutral-atmosphere between 150 and 500 km, Space Research XIII:349-355.
7. Barlier, F., Bauer, P., Jaeck, C., Thuillier, G., and Kockharts, G. (1974) North-south asymmetries in the thermosphere during the last maximum of the solar cycle, J. Geophys. Res. 79:5273-5285.
8. Forbes, J.M., Marcos, F.A., and Champion, K.S.W. (1977) Lower thermosphere response to geomagnetic activity, Space Res. XVIII:173-176.
9. Rice, C.J., and Sharp, L.R. (1977) Neutral Atmospheric Waves in the Thermosphere and Tropospheric Weather System, SAMSO-TR-77-98.
10. Philbrick, C.R., and McIsaac, J.P. (1972) Measurements of atmospheric composition near 400 km, Space Research XVI:743-749.
11. Ching, B.K., and Carter, V.L. (1974) Ion gauge measurements of latitudinal density variations at night, Geophys. Res. Lett. 1:93-96.

12. Hong, S.S., and Lindzen, R.S. (1976) Solar semidiurnal tide in the thermosphere, J. Atmos. Sci. 33:135-153.

13. Marcos, F.A., McInerney, R.E., and Fioretti, R.W. (1978) Variability of the Lower Thermosphere Determined From Satellite Accelerometer Data, AFGL-TR-78-0134, AD A058-982.

Appendix A

Histograms of Frequency Distributions of Ratios of Measurements/Jacchia 71 Model

Number	Altitude Range	Latitude Range	K_p Range
A1	Perigee to 300 km	90°N to 90°S	0 to 9
A2	"	90°N to 0°	"
A3	"	90°S to 0°	"
A4	"	90°N to 0°	5 to 9
A5	"	90°S to 0°	"
A6	250 Km to 300 km	90°N to 0°	3 to 5
A7	"	90°S to 0°	"
A8	"	15°N to 0°	0 to 3
A9	"	15°S to 0°	"
A10	"	30°N to 15°N	5 to 9
A11	"	30°S to 15°S	"
A12	"	60°N to 45°N	3 to 5
A13	"	60°S to 45°S	"
A14	200 Km to 250 km	15°N to 0°	"
A15	"	15°S to 0°	"
A16	"	75°N to 60°N	5 to 9
A17	"	75°S to 60°S	"
A18	"	90°N to 75°N	3 to 5
A19	"	90°S to 75°S	"
A20	Perigee to 200 km	30°N to 15°N	5 to 9
A21	"	30°S to 15°S	"
A22	"	45°N to 30°N	3 to 5
A23	"	45°S to 30°S	"
A24	"	75°N to 60°N	0 to 3
A25	"	75°S to 60°S	"
A26	"	90°N to 75°N	3 to 5
A27	"	90°S to 75°S	"

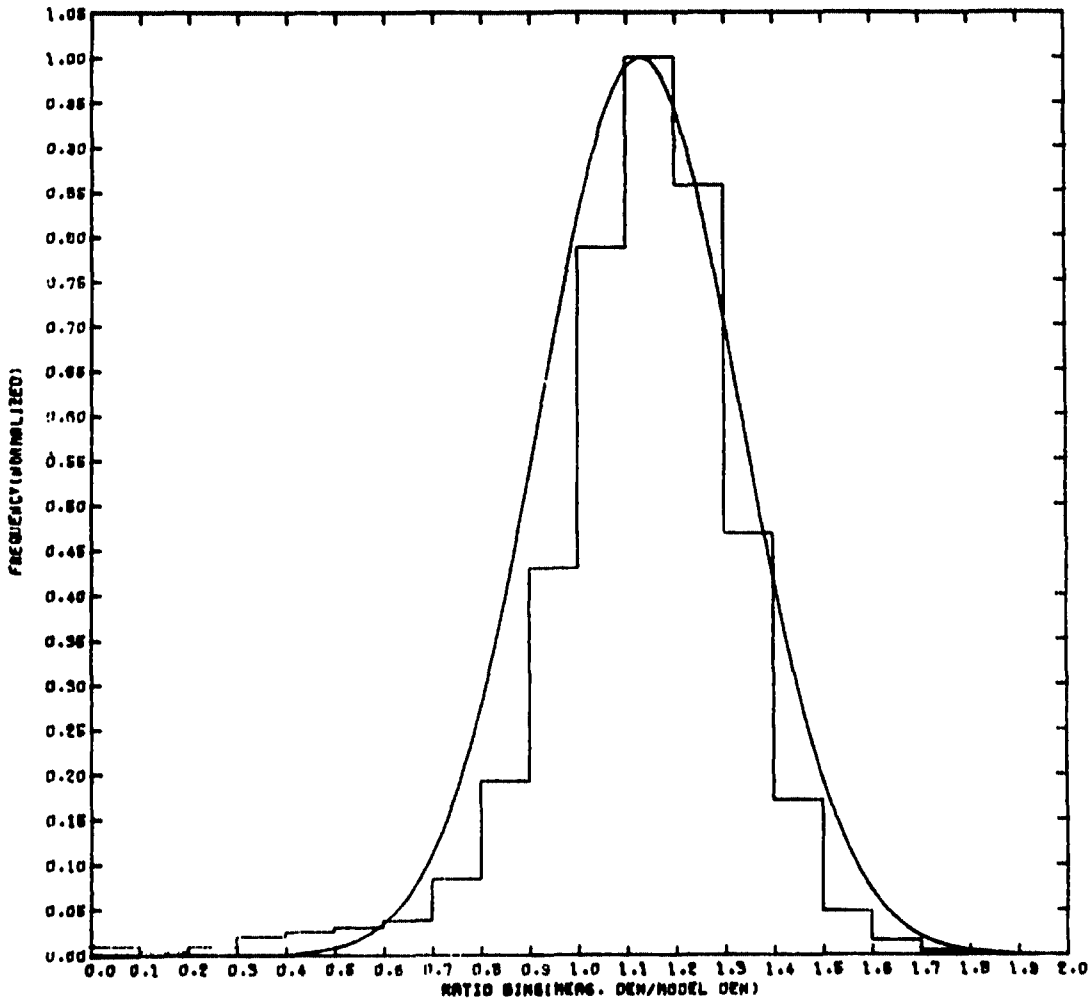
100 DATA
KP LIMITS 0.0- 9.0
ALTLIM 0.- 300.
LAT LIM -90.- 90.
BOTH HEMISPHERES
MAX Y VAL 36892.00
MEAN VALUE 1.13
ST. DEV. 2.05E-01
TOTAL POINTS= 154584
FREQUENCY(NORMALIZED)
1.05
1.00
0.95
0.90
0.85
0.80
0.75
0.70
0.65
0.60
0.55
0.50
0.45
0.40
0.35
0.30
0.25
0.20
0.15
0.10
0.05
0.00
0.0 0.1 0.2 0.3 0.4 0.5 0.6 0.7 0.8 0.9 1.0 1.1 1.2 1.3 1.4 1.5 1.6 1.7 1.8 1.9 2.0
RATIO BINS(MEAS. DEN/MODEL DEN)

Number A1

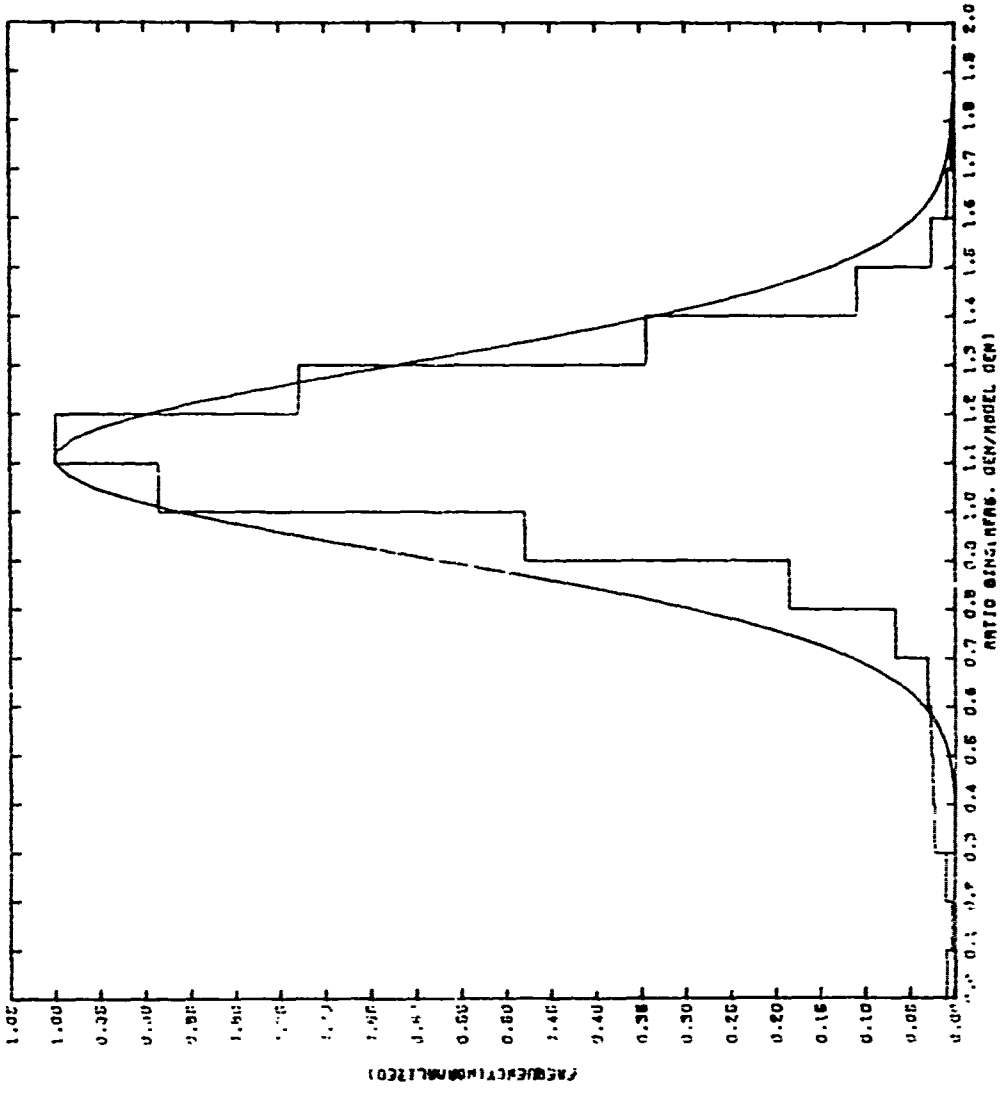
1.00
0.95
0.90
0.85
0.80
0.75
0.70
0.65
0.60
0.55
0.50
0.45
0.40
0.35
0.30
0.25
0.20
0.15
0.10
0.05
0.0
0.1 0.2 0.3 0.4 0.5 0.6 0.7 0.8 0.9 1.0 1.1 1.2 1.3 1.4 1.5 1.6 1.7 1.8 1.9 2.0
RATIO BINGHAM. OEM/MODEL OEM)
FREQUENCY(NORMALIZED)
ODD ORTH
NP LIMITS 0.0- 0.1
AL LIM 0.- 300.
LAT LIM 0.- 80.
NORTHERN HEMISPHERE
MAX Y VAL 93186.00
MEAN VALUE 1.11
ST. DEV. 1.97E-01
TOTAL POINTS 91329

Number A2

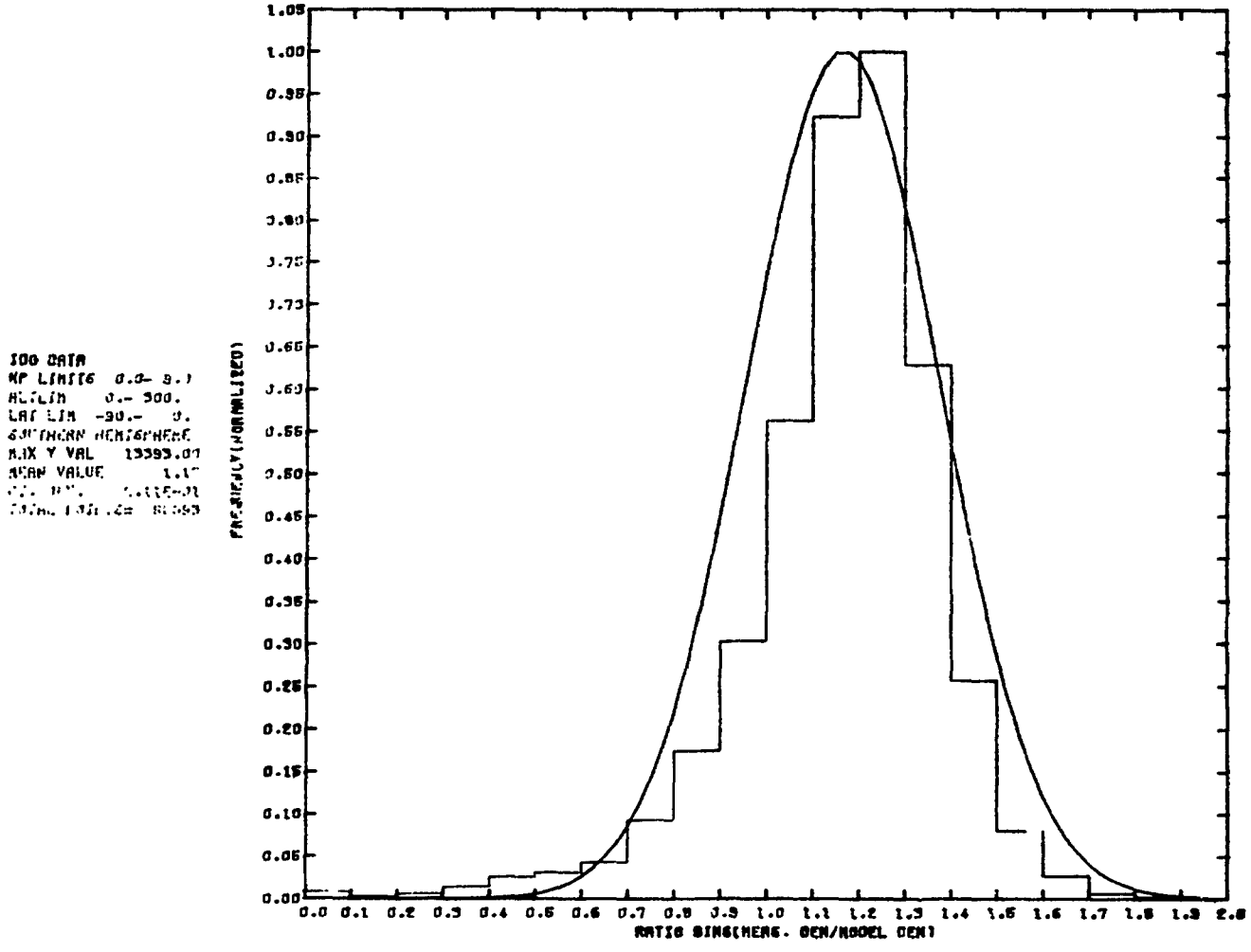
100 DATA
MP LIMITS 0.0- 8.)
ALT LIM 0.- 500.
LAT LIM -90.- 0.
SOUTHERN HEMISPHERE
MAX Y VAL 13393.01
MEAN VALUE 1.1
FREQUENCY(NORMALIZED)
RATIO BINS(MEAS. OEN/MODEL OEN)

Number A3

IDB DATA
KP LIMITS 5.0- 8.0
ALTLIM 0.- 300.
LAT LIM 0.- 90.
NORTHERN HEMISPHERE
MAX Y VAL 1159.00
MEAN VALUE 1.06
ST. DEV. 1.[illegible]E-1
TOTAL POINTS= 4478

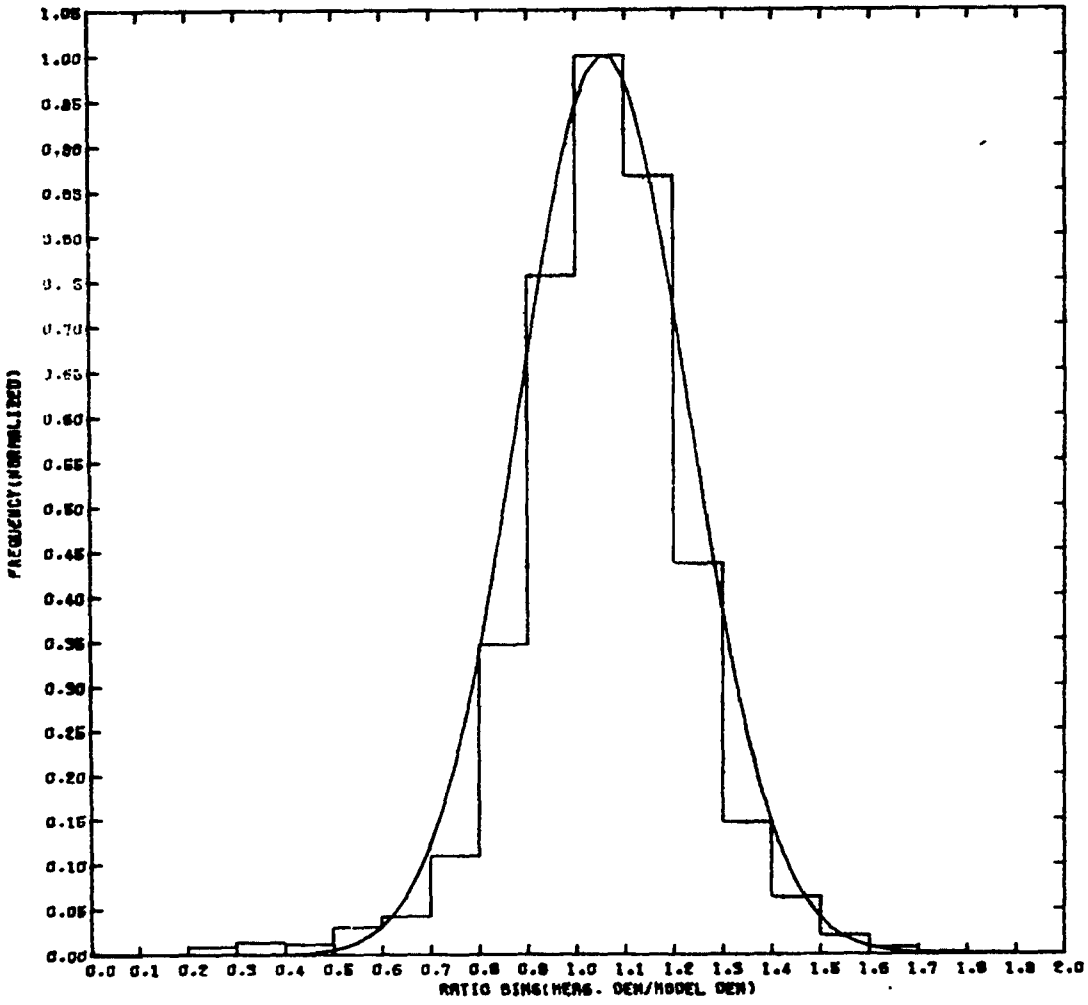

Number A4

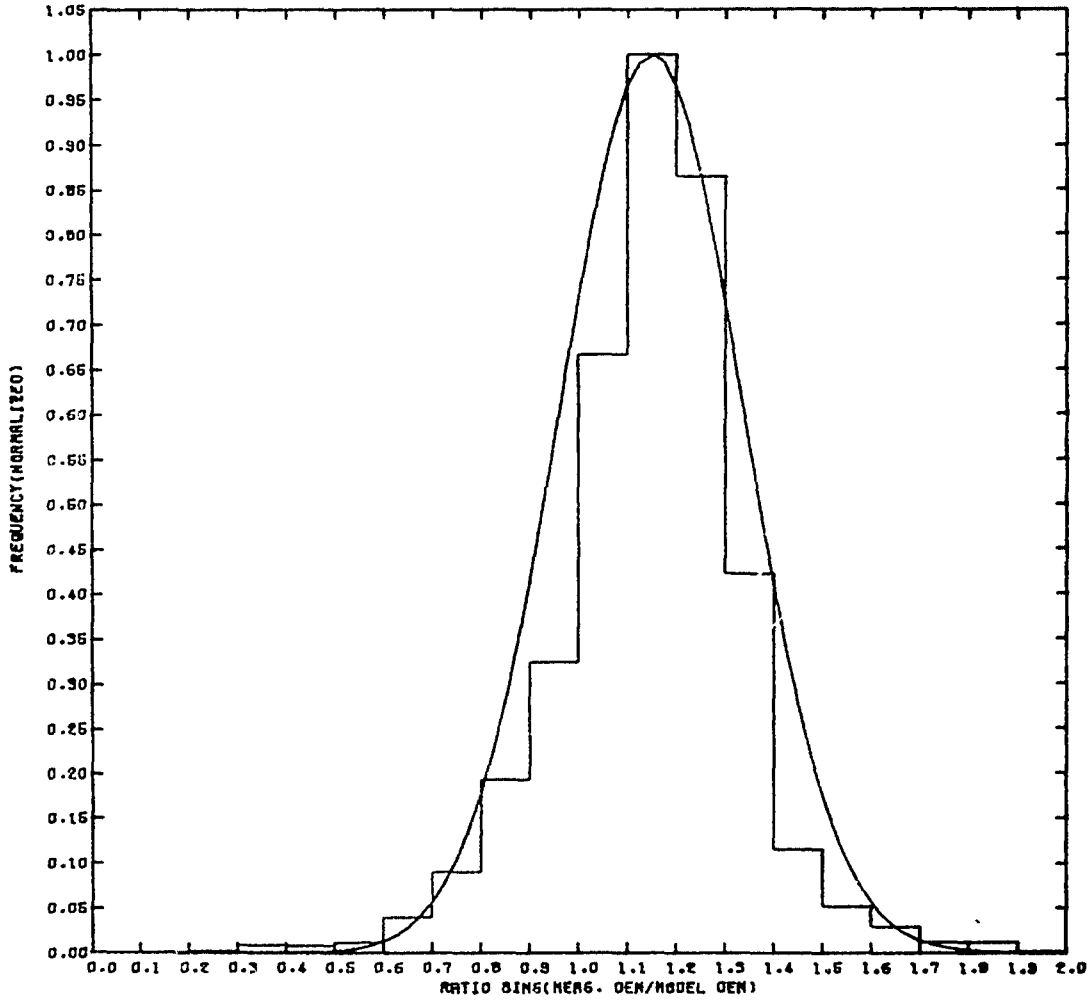
IDB DATA
KP LIMITS 5.0- 5.0
ALTLIM 0.- 900.
LAT LIM -80.- 0.
SOUTHERN HEMISPHERE
MAX Y VAL 682.00
MEAN VALUE 1.15
ST. DEV. 1.88E-01
TOTAL POINTS= 2238
FREQUENCY(NORMALIZED)
RATIO BINS(MEAS. DEN/MODEL DEN)

Number A5

IDB DATA
KP LIMITS 3.0- 5.0
ALTLIM 250.- 300.
LAT LIM 0.- 80.
NORTHERN HEMISPHERE
MAX Y VAL 1339.00
MEAN VALUE 1.03
ST. DEV. 2.07E-01
TOTAL POINTS= 6880

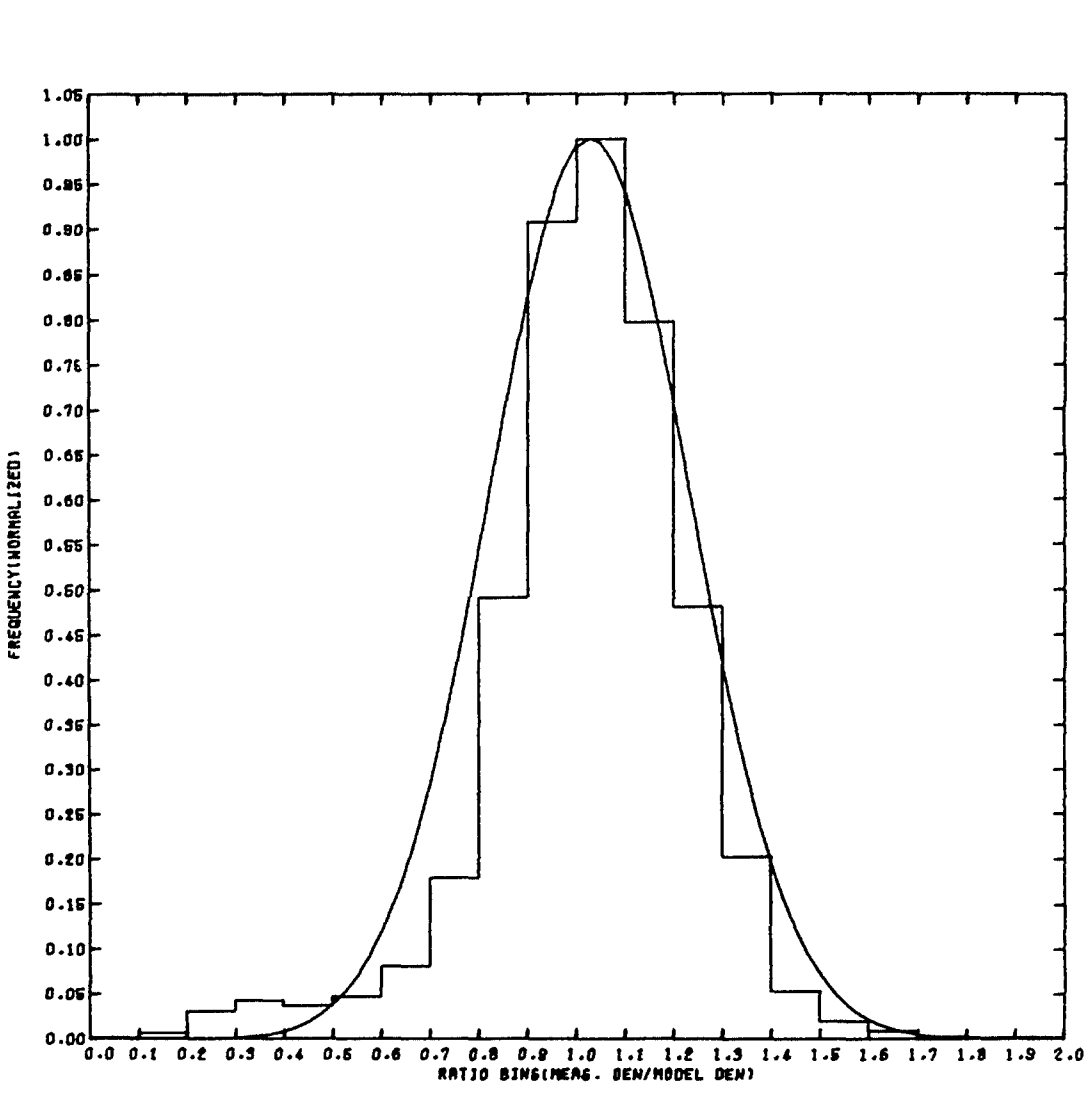

Number A6

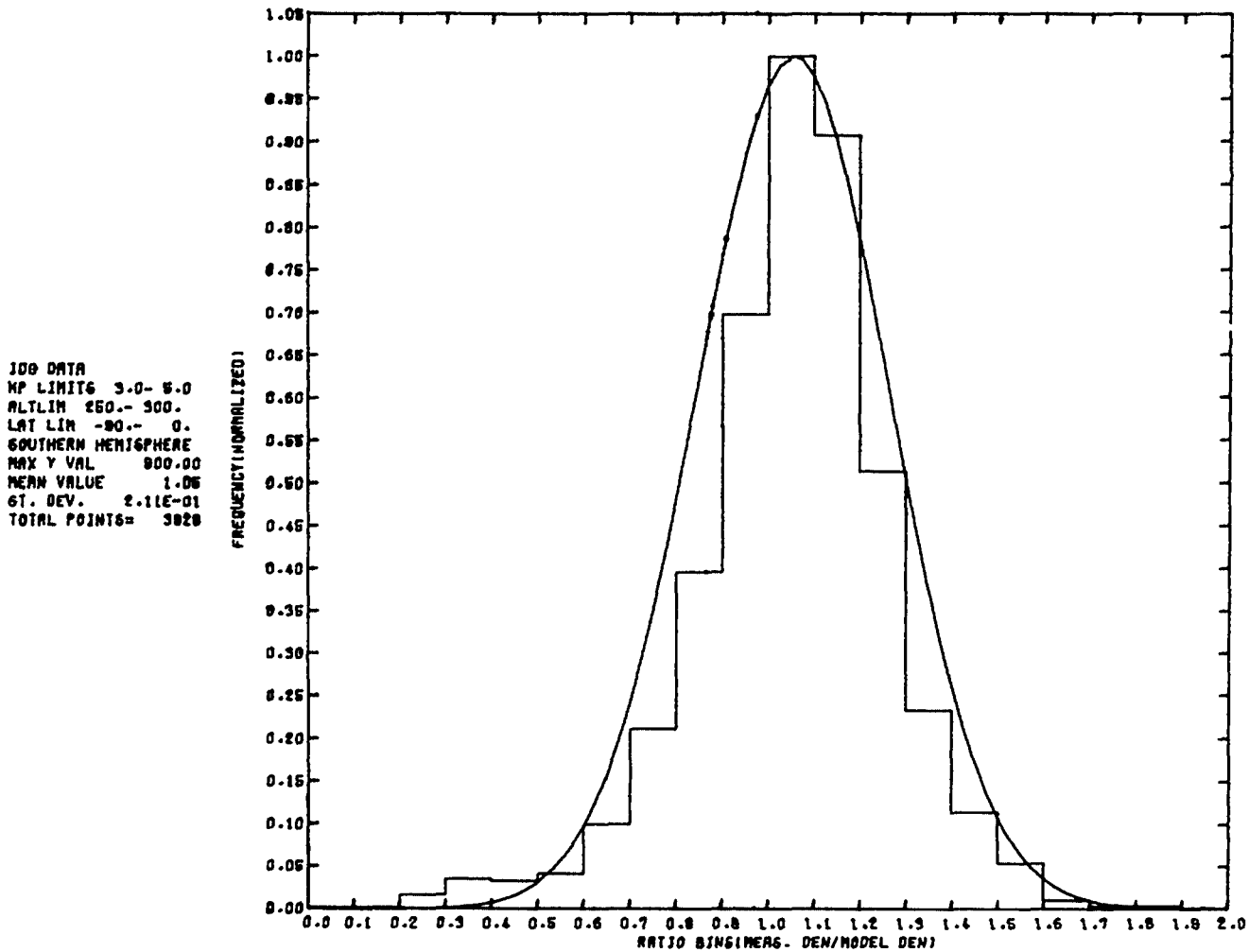
IDB DATA
KP LIMITS 3.0- 5.0
ALTLIM 250.- 300.
LAT LIM -90.- 0.
SOUTHERN HEMISPHERE
MAX Y VAL 900.00
MEAN VALUE 1.06
ST. DEV. 2.11E-01
TOTAL POINTS= 3928
FREQUENCY(NORMALIZED)
1.00
0.95
0.90
0.85
0.80
0.75
0.70
0.65
0.60
0.55
0.50
0.45
0.40
0.35
0.30
0.25
0.20
0.15
0.10
0.05
0.00
0.0 0.1 0.2 0.3 0.4 0.5 0.6 0.7 0.8 0.9 1.0 1.1 1.2 1.3 1.4 1.5 1.6 1.7 1.8 1.9 2.0
RATIO BINS(MEAS. DEN/MODEL DEN)

Number A7

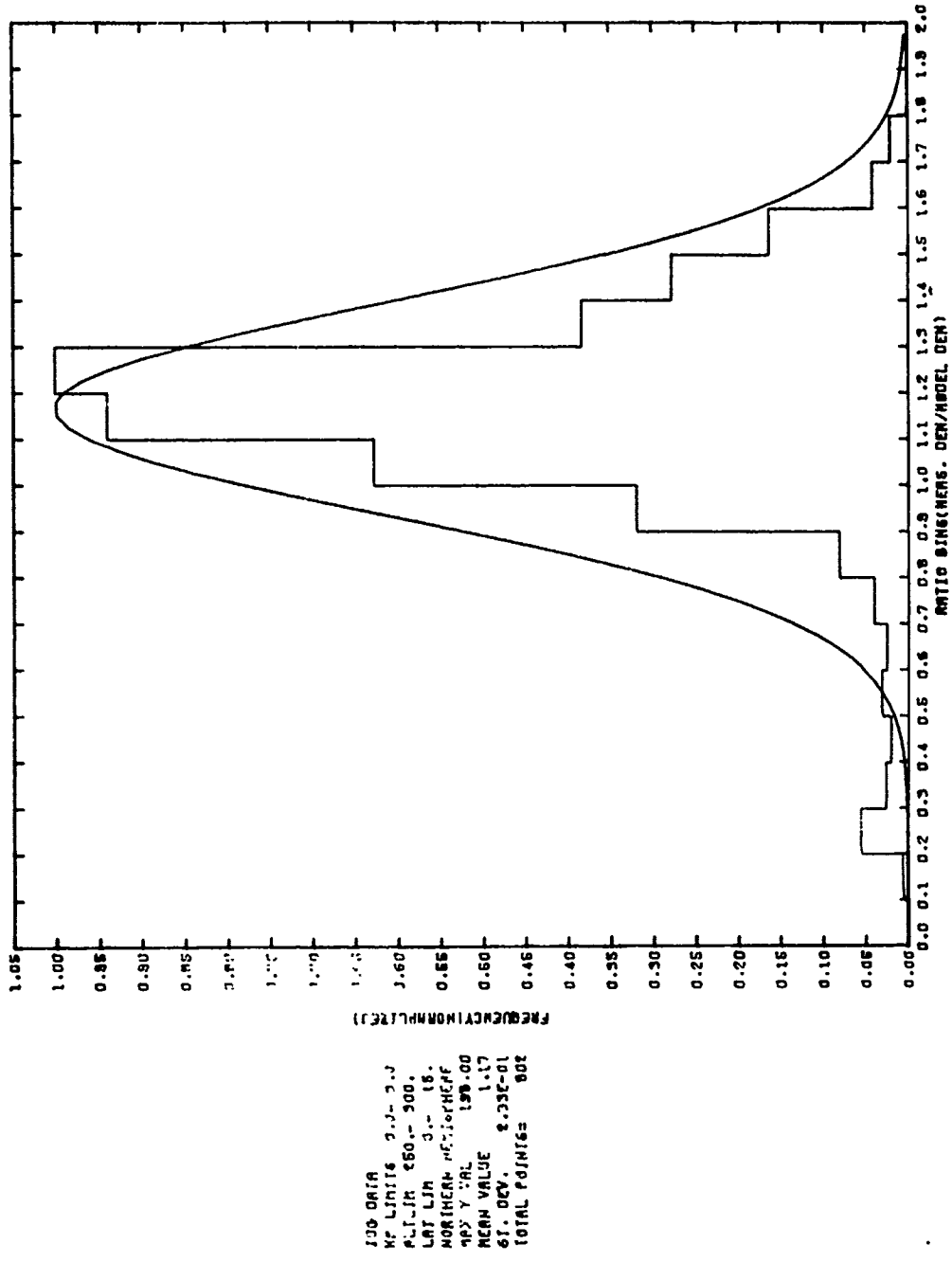
FREQUENCY(NORMALIZED)
RATIO ENGINEERS. DEN/MODEL DEN)
0.0 0.1 0.2 0.3 0.4 0.5 0.6 0.7 0.8 0.9 1.0 1.1 1.2 1.3 1.4 1.5 1.6 1.7 1.8 1.9 2.0
1.05 1.00 0.95 0.90 0.85 0.80 0.75 0.70 0.65 0.60 0.55 0.50 0.45 0.40 0.35 0.30 0.25 0.20 0.15 0.10 0.05 0.00
MEAN VALUE 1.17
TOTAL POINTS= 802

Number A8

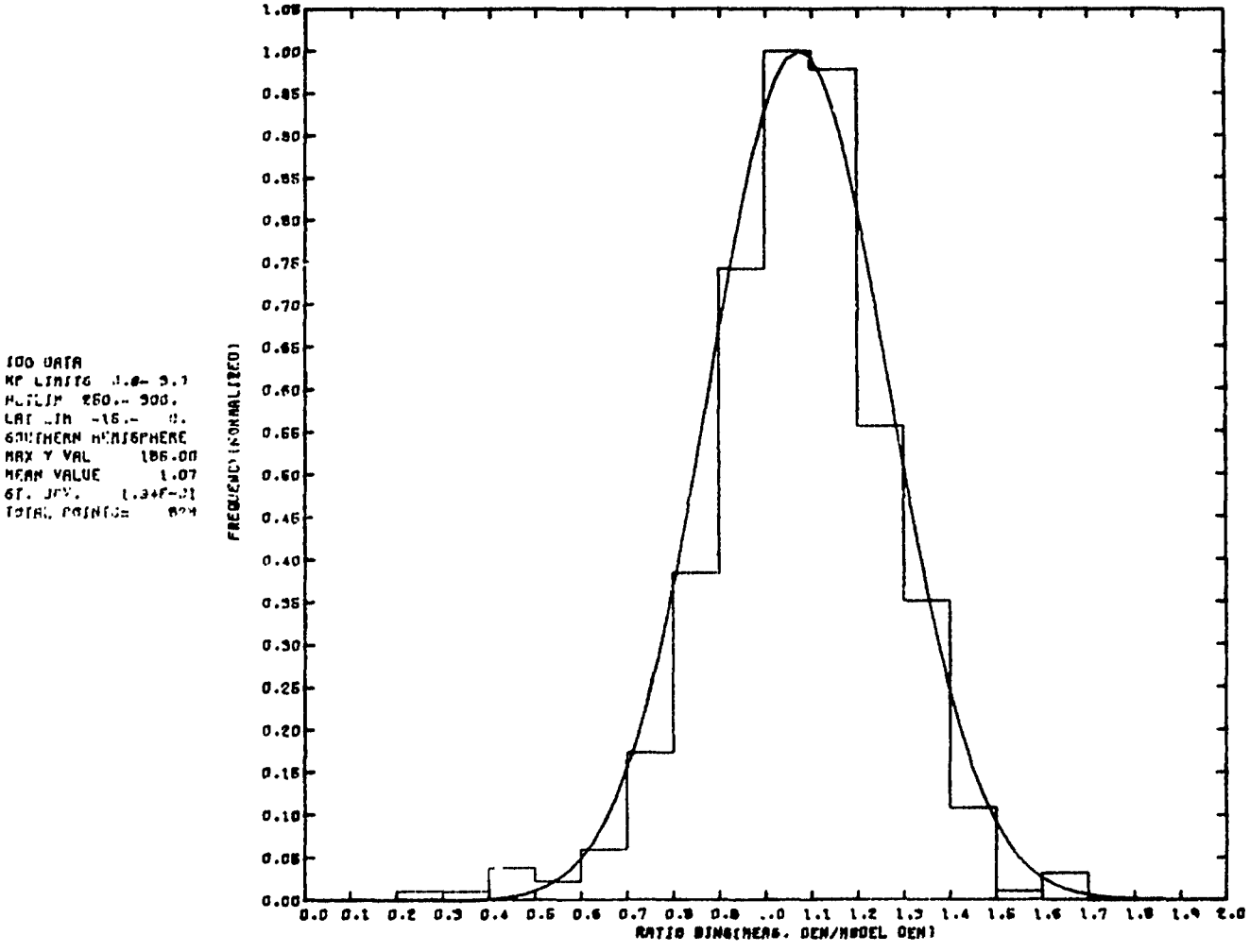
ISO DATA
MF LIMITS 3.0- 5.1
PRESS 250.- 900.
LAT LIM -15.- 0.
SOUTHERN HEMISPHERE
MAX Y VAL 186.00
MEAN VALUE 1.07
ST. DEV. 1.34E-01
TOTAL POINTS= 824
FREQUENCY (NORMALIZED)
1.05
1.00
0.95
0.90
0.85
0.80
0.75
0.70
0.65
0.60
0.55
0.50
0.45
0.40
0.35
0.30
0.25
0.20
0.15
0.10
0.05
0.00
0.0 0.1 0.2 0.3 0.4 0.5 0.6 0.7 0.8 0.9 1.0 1.1 1.2 1.3 1.4 1.5 1.6 1.7 1.8 1.9 2.0
RATIO BIN(MEAS. DEN/MODEL DEN)

Number A9

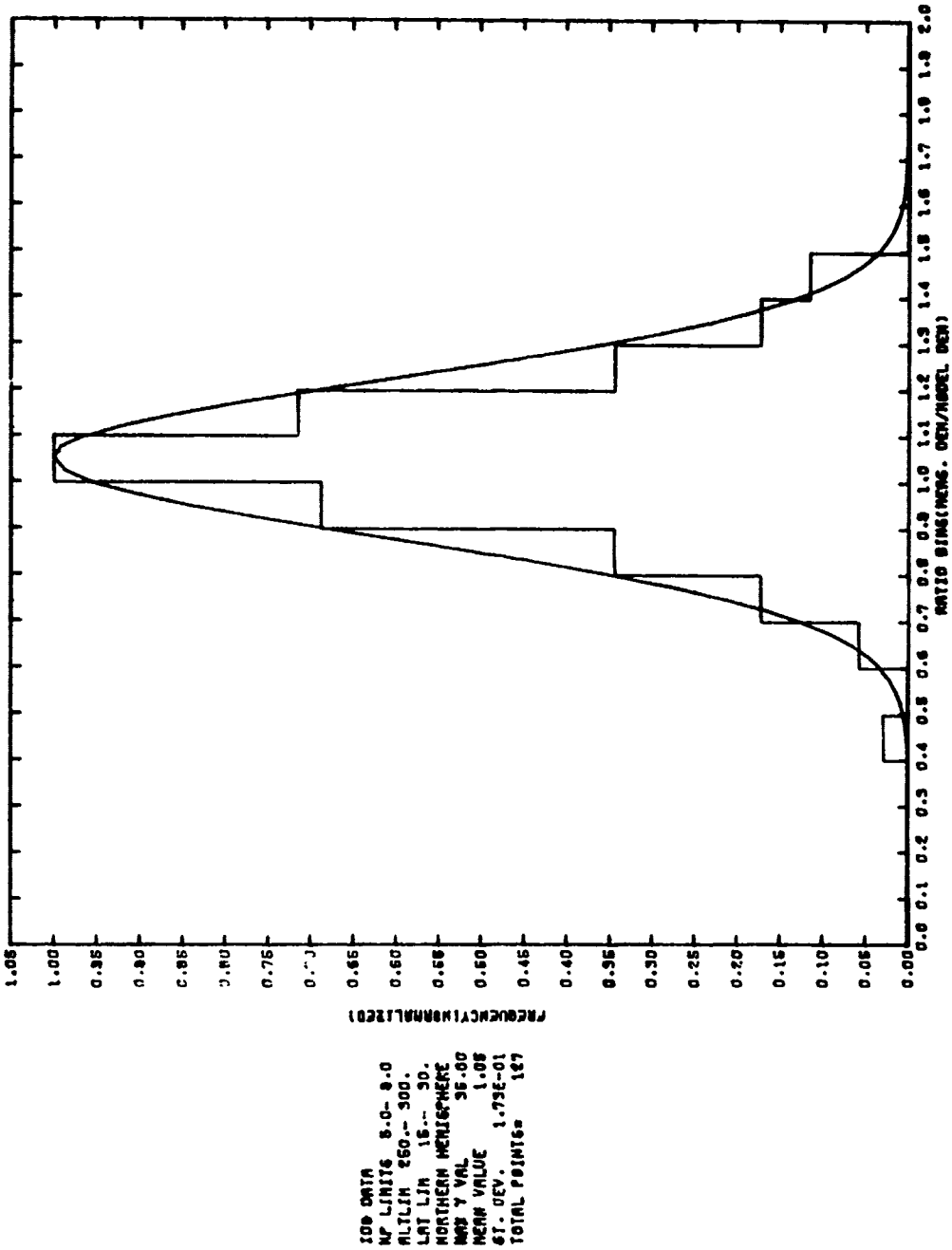
FREQUENCY(NORMALIZED)
RATIO SIMG(MEAS. OEN/MODEL OEN)
IOD DATA
NF LIMITS 8.0- 8.0
ALTLIM 250.- 300.
LAT LIM 15.- 30.
NORTHERN HEMISPHERE
NUM Y VAL 36.00
MEAN VALUE 1.08
ST. DEV. 1.73E-01
TOTAL POINTS= 127

Number A10

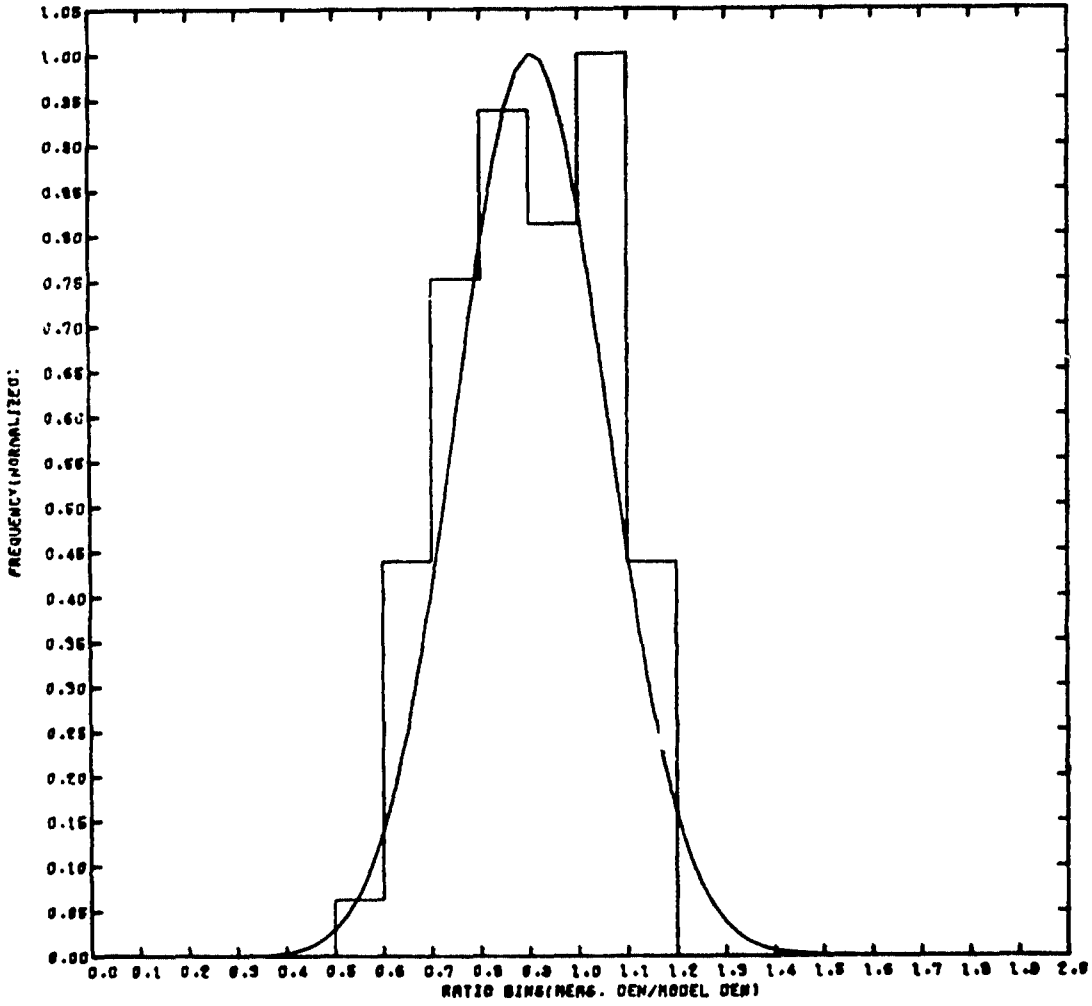
100 UNIT
MEAN VALUE .80
ST. DEV. 1.84E-01
TOTAL POINTS= 71
SOLINCAN HEMISPHERE
MAX Y VAL 16.00
FREQUENCY(NORMALIZED)
RATIO BINS(MEAS. OEN/MODEL OEN)

Number A11

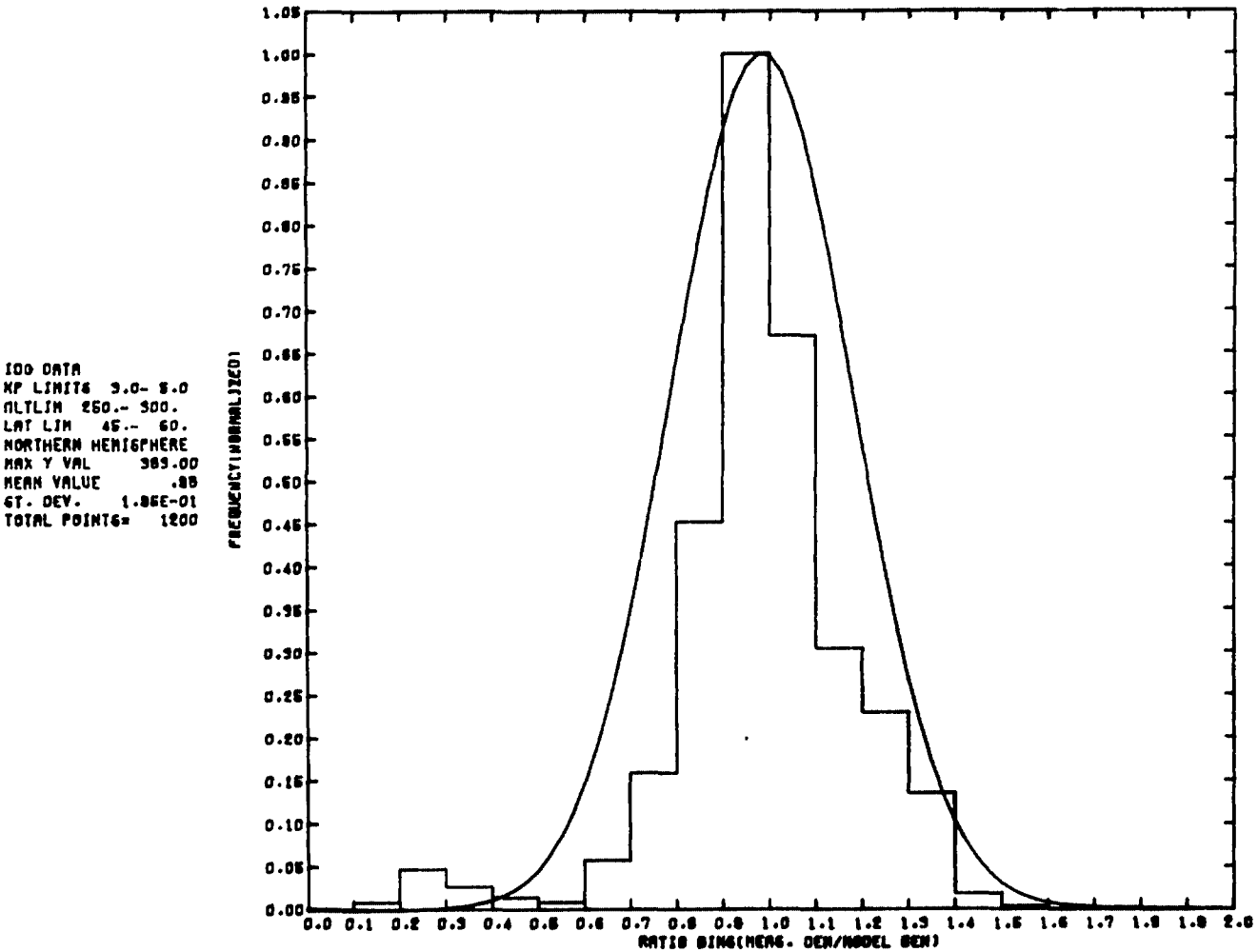
IDD DATA
KP LIMITS 3.0- 5.0
ALTLIM 250.- 300.
LAT LIM 45.- 60.
NORTHERN HEMISPHERE
MAX Y VAL 389.00
MEAN VALUE .88
ST. DEV. 1.86E-01
TOTAL POINTS= 1200
FREQUENCY(NORMALIZED)
1.05
1.00
0.95
0.90
0.85
0.80
0.75
0.70
0.65
0.60
0.55
0.50
0.45
0.40
0.35
0.30
0.25
0.20
0.15
0.10
0.05
0.00
0.0 0.1 0.2 0.3 0.4 0.5 0.6 0.7 0.8 0.9 1.0 1.1 1.2 1.3 1.4 1.5 1.6 1.7 1.8 1.9 2.0
RATIO BINS(MEAS. DEN/MODEL DEN)

Number A12

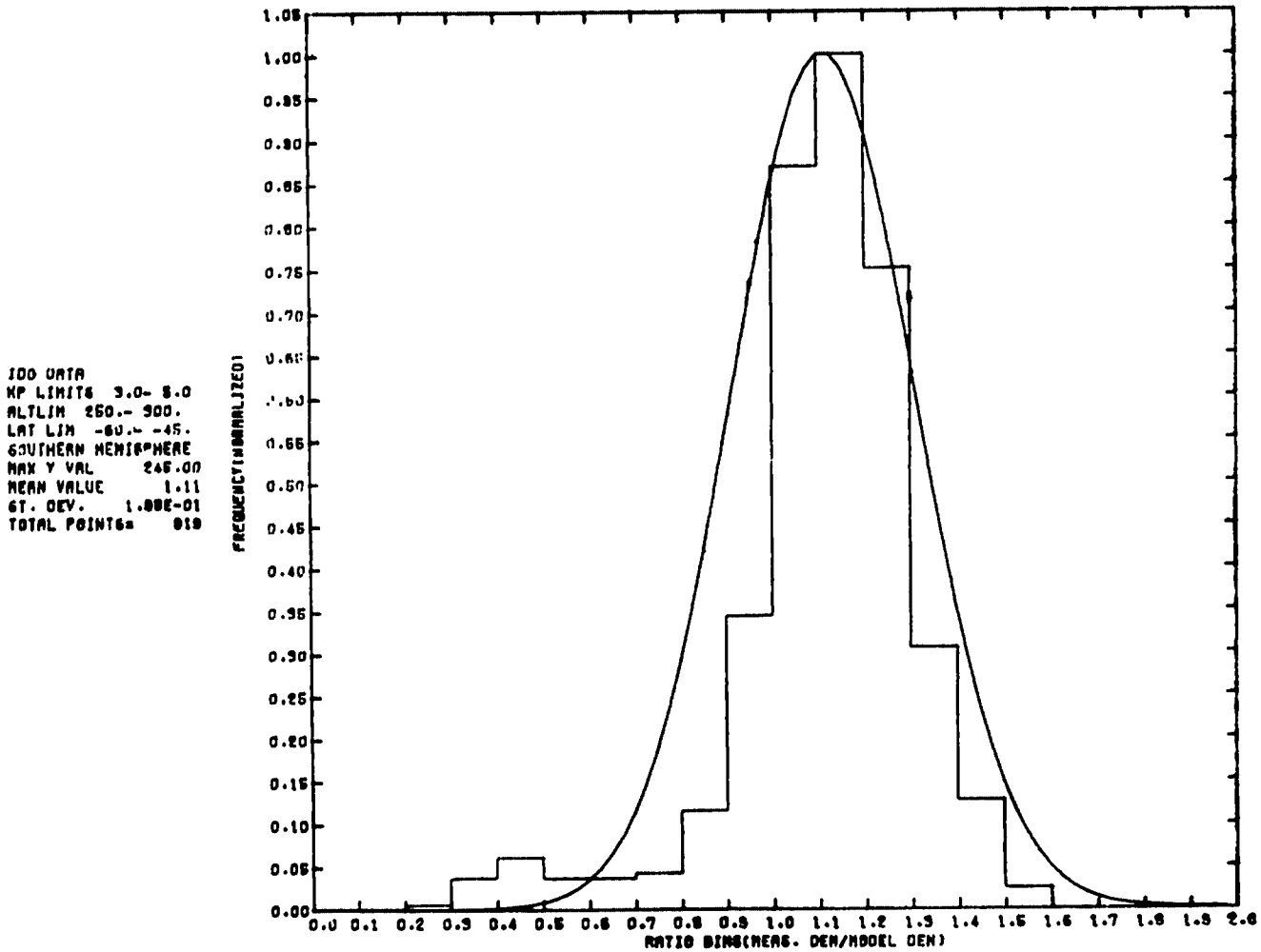
100 DATA
KP LIMITS 3.0- 5.0
ALTLIM 250.- 300.
LAT LIM -80.- -45.
SOUTHERN HEMISPHERE
MAX Y VAL 246.00
MEAN VALUE 1.11
ST. DEV. 1.00E-01
TOTAL POINTS= 919
FREQUENCY(NORMALIZED)
1.05
1.00
0.95
0.90
0.85
0.80
0.75
0.70
0.65
0.60
0.55
0.50
0.45
0.40
0.35
0.30
0.25
0.20
0.15
0.10
0.05
0.00
0.0 0.1 0.2 0.3 0.4 0.5 0.6 0.7 0.8 0.9 1.0 1.1 1.2 1.3 1.4 1.5 1.6 1.7 1.8 1.9 2.0
RATIO BINS(MEAS. DEN/MODEL DEN)

Number A13

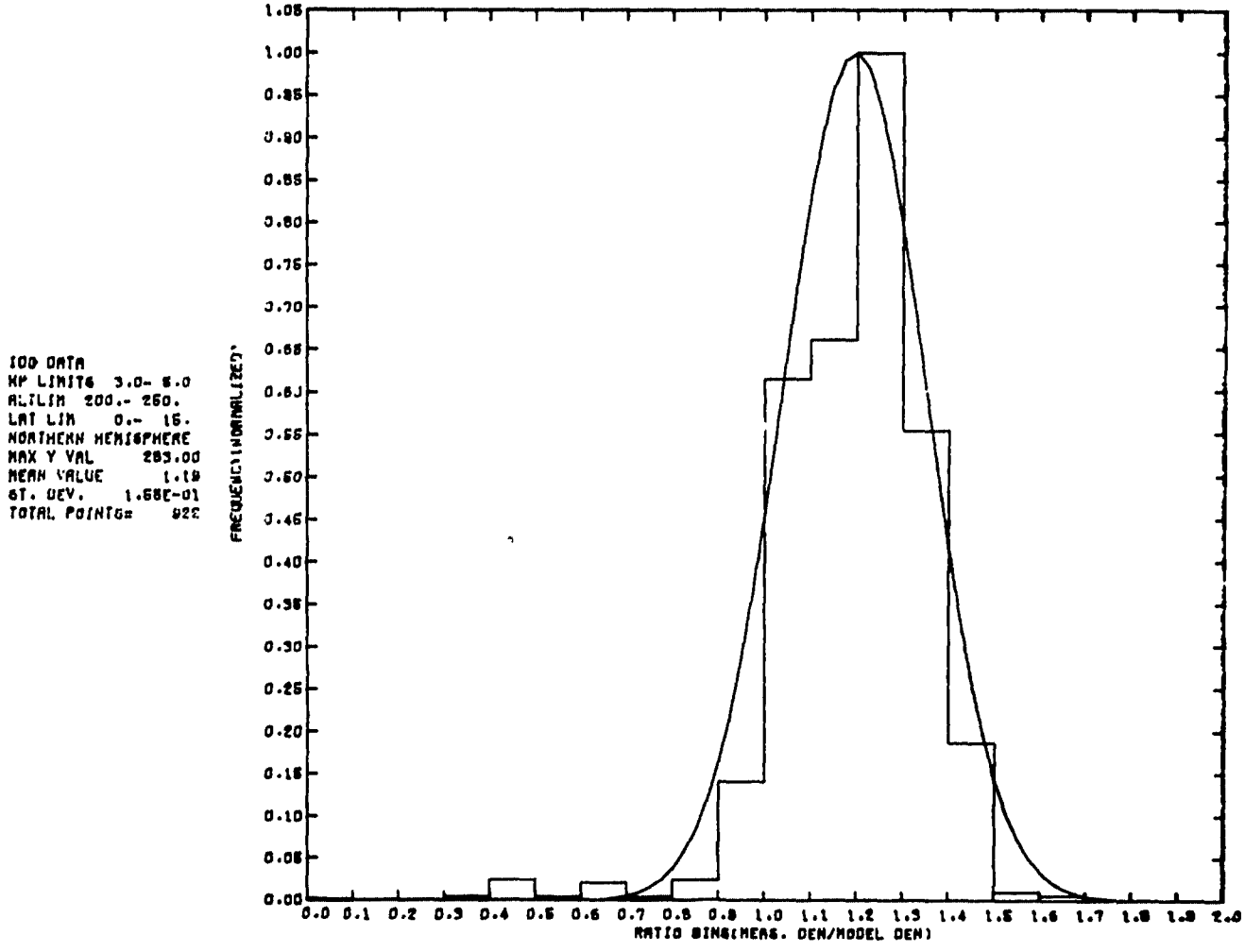
IDD DATA
KP LIMITS 3.0- 5.0
ALTLIM 200.- 250.
LAT LIM 0.- 15.
NORTHERN HEMISPHERE
MAX Y VAL 283.00
MEAN VALUE 1.19
ST. DEV. 1.68E-01
TOTAL POINTS= 922
FREQUENCY(NORMALIZED)
RATIO BINS(MEAS. DEN/MODEL DEN)

Number A14

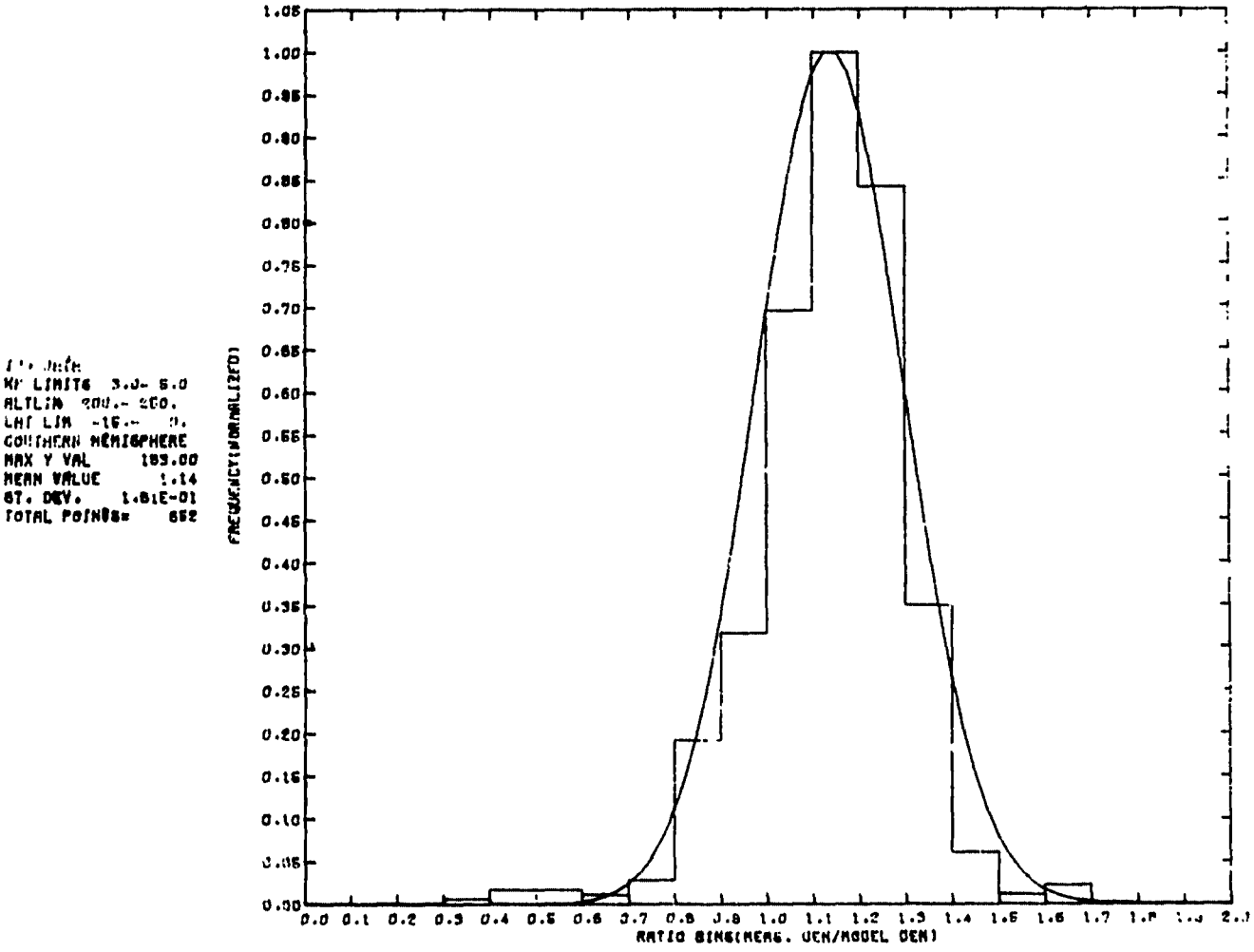
KP LIMITS 3.0- 6.0
ALTLIM 200.- 200.
LAT LIM -16.- 0.
SOUTHERN HEMISPHERE
MAX Y VAL 183.00
MEAN VALUE 1.14
ST. DEV. 1.81E-01
TOTAL POINTS= 852
FREQUENCY(NORMALIZED)
RATIO BINS(MEAS. DEN/MODEL DEN)

Number A15

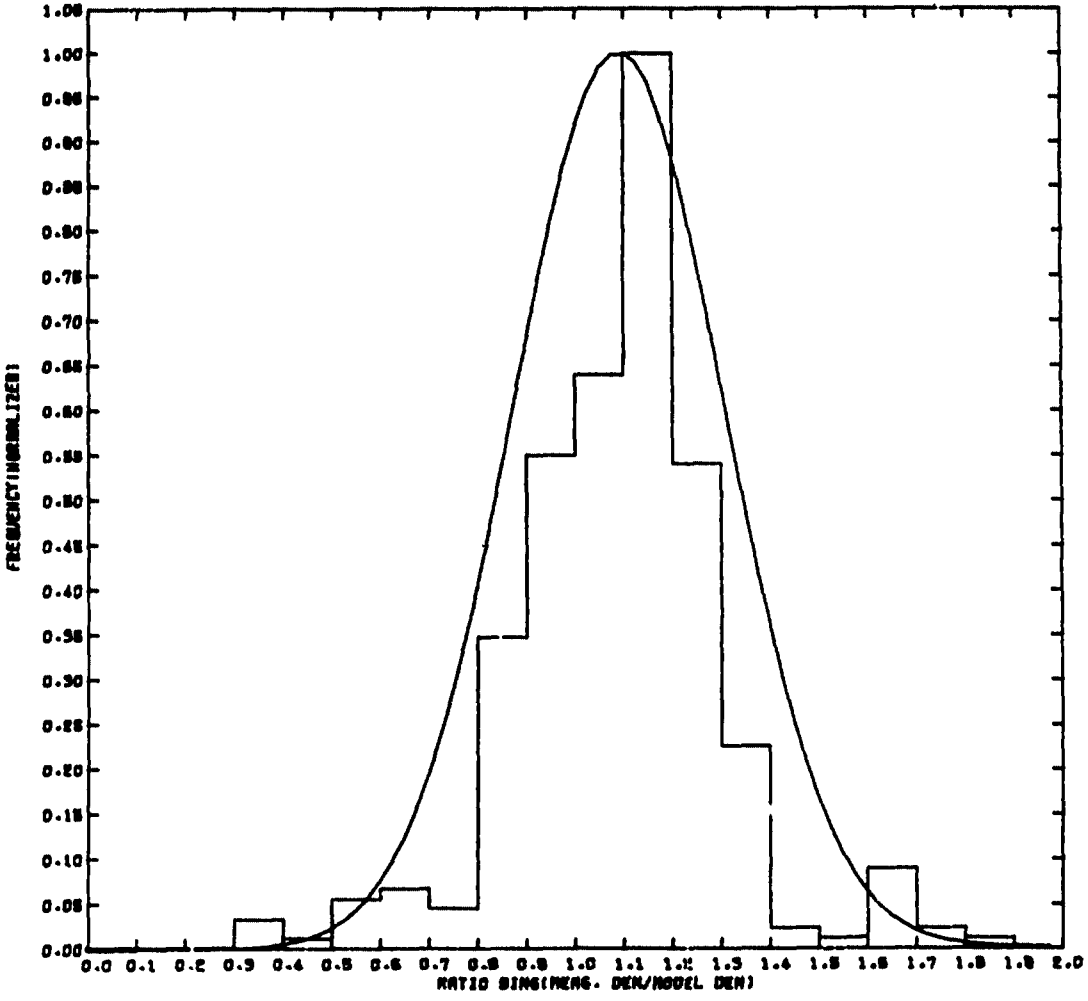
IDB DATA
HF LIMITS 8.0- 9.0
ALTLIM 200.- 250.
LAT LIM 60.- 75.
NOR/MERN HEMISPHERE
MAX Y VAL 98.00
MEAN VALUE 1.00
ST. DEV. 2.16E-01
TOTAL POINTS= 327
FREQUENCY(NORMALIZED)
RATIO SING(MEAS. DEN/MODEL DEN)

Number A16

IDG DATA
KP LIMITS 5.0- 8.0
ALTLIM 200.- 250.
LAT LIM -75.- -60.
SOUTHERN HEMISPHERE
MAX Y VAL 10.00
MEAN VALUE 1.51
ST. DEV. 9.58E-02
TOTAL POINTS= 29

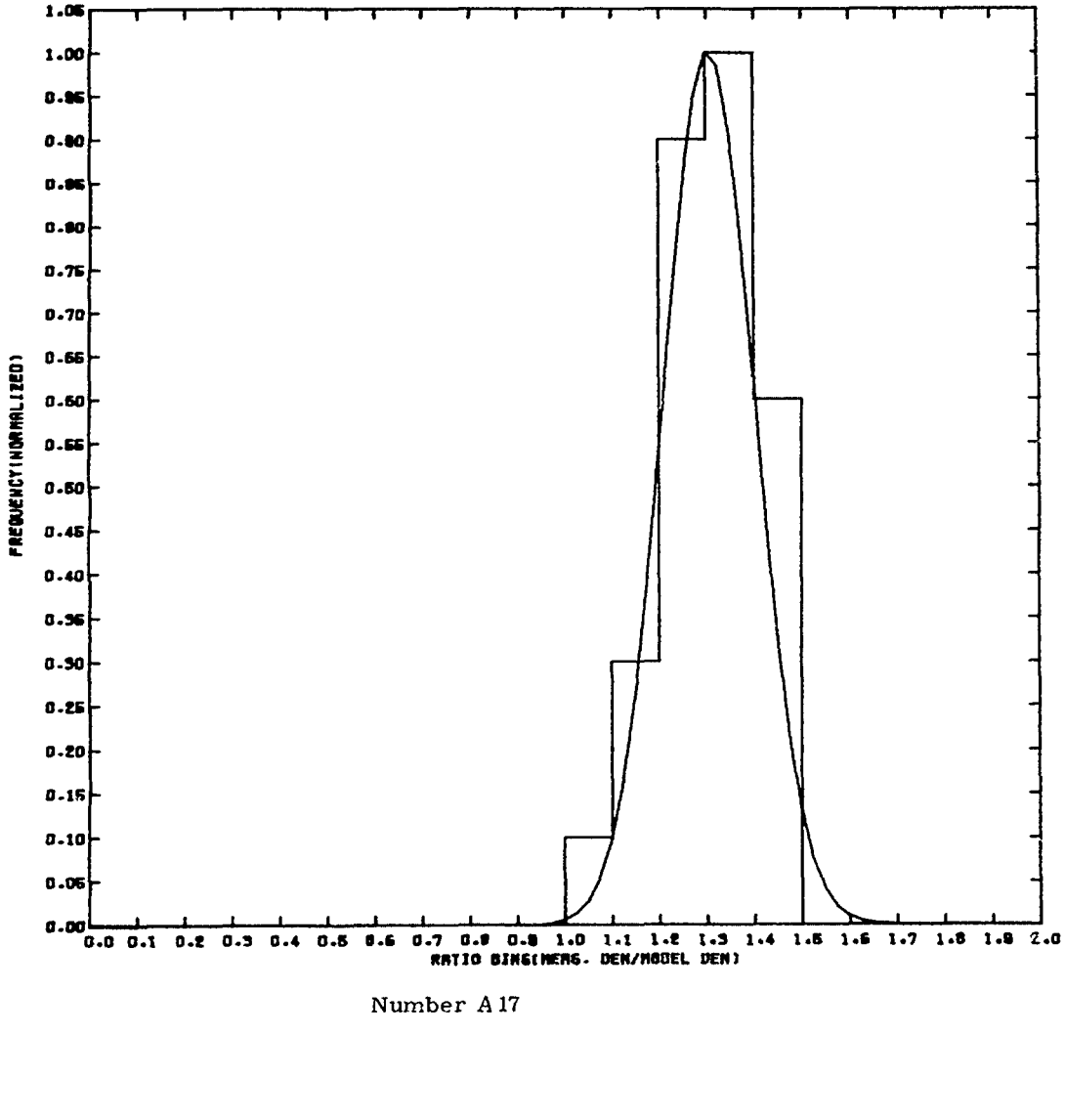

Number A 17

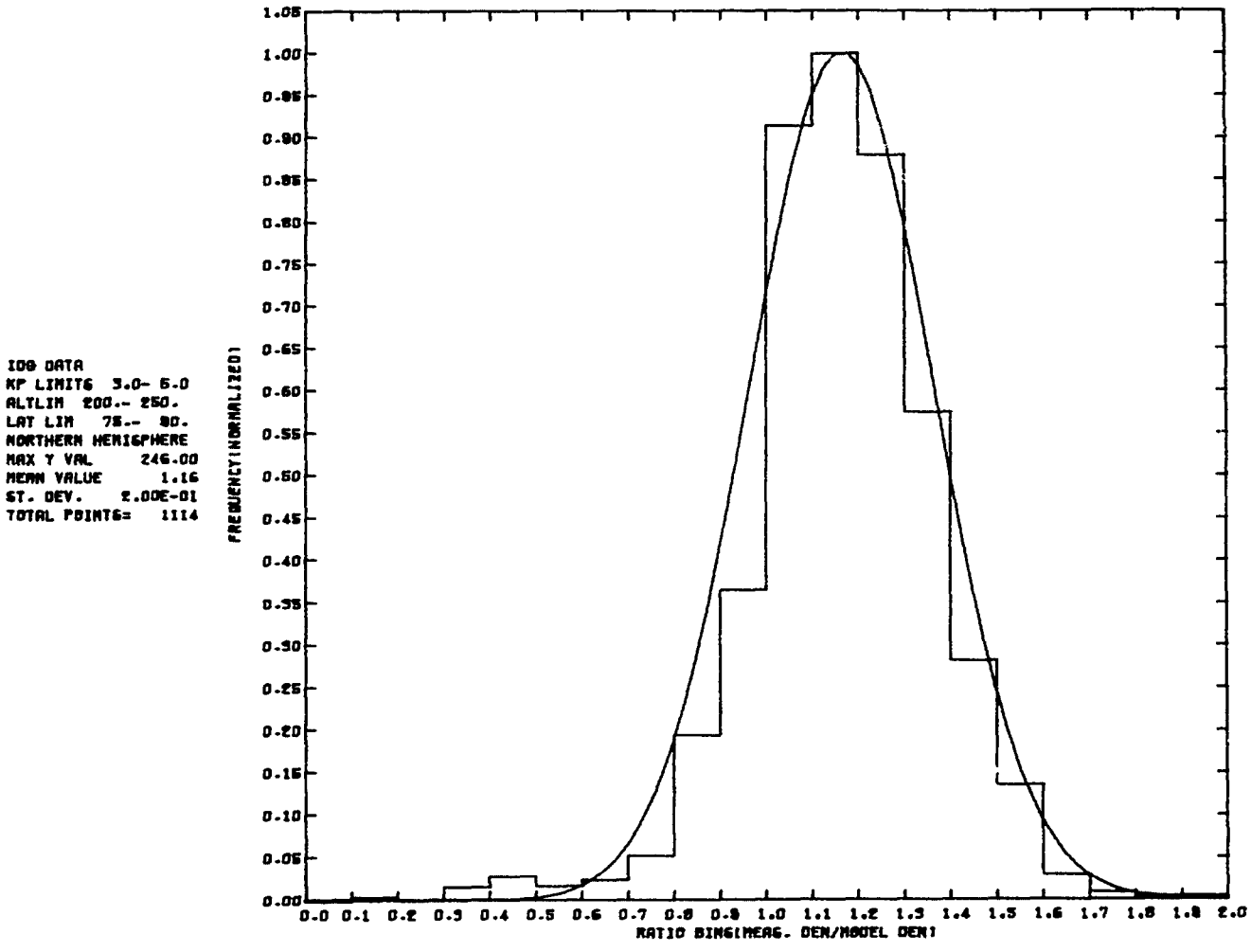
IDB DATA
KP LIMITS 3.0- 6.0
ALTLIM 200.- 250.
LAT LIM 75.- 90.
NORTHERN HEMISPHERE
MAX Y VAL 246.00
MEAN VALUE 1.16
ST. DEV. 2.00E-01
TOTAL POINTS= 1114
FREQUENCY(NORMALIZED)
RATIO BINS(MEAS. DEN/MODEL DEN)

Number A18

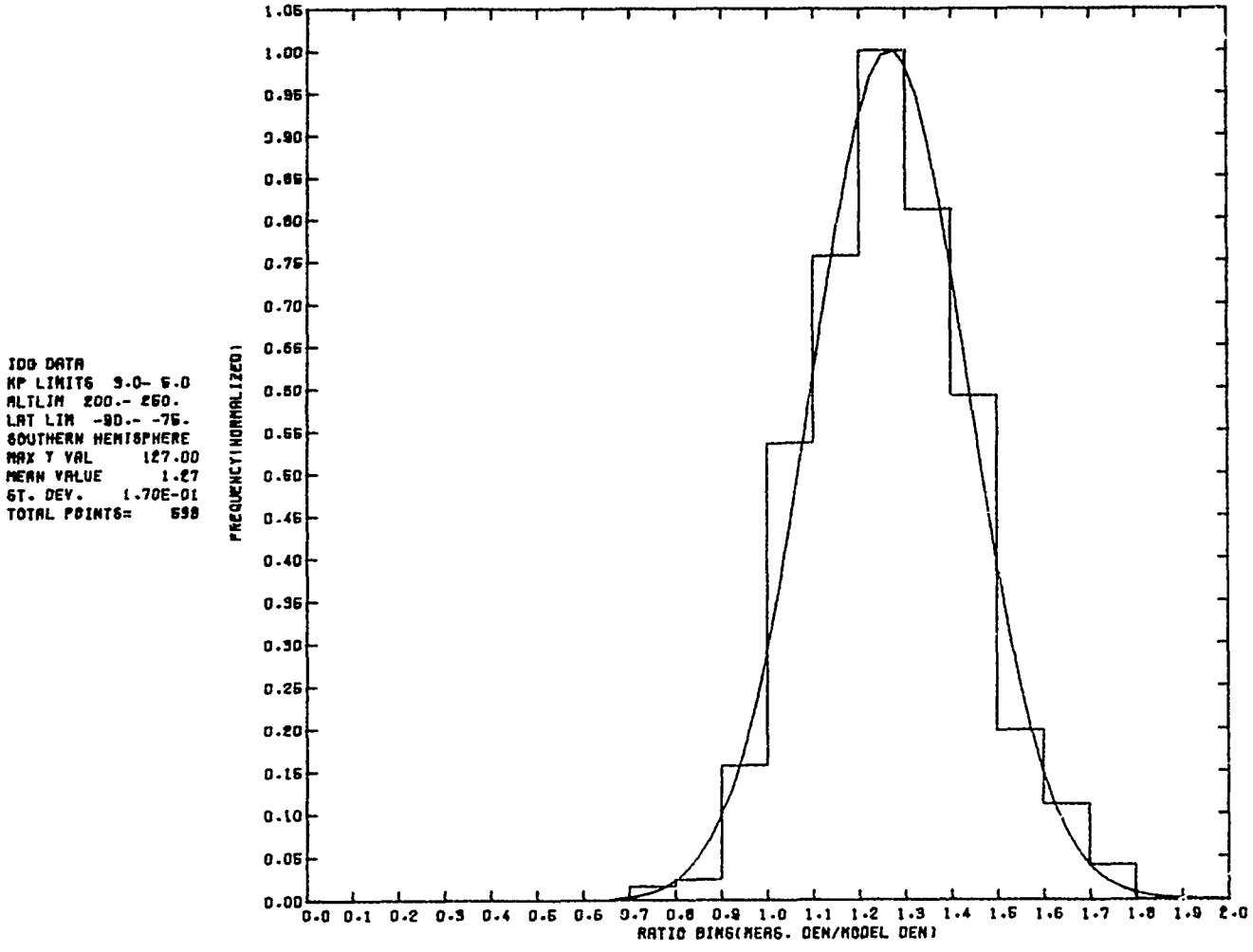
IDD DATA
KP LIMITS 3.0- 5.0
ALTLIM 200.- 250.
LAT LIM -90.- -75.
SOUTHERN HEMISPHERE
MAX Y VAL 127.00
MEAN VALUE 1.27
ST. DEV. 1.70E-01
TOTAL POINTS= 598
FREQUENCY(NORMALIZED)
1.05
1.00
0.95
0.90
0.85
0.80
0.75
0.70
0.65
0.60
0.55
0.50
0.45
0.40
0.35
0.30
0.25
0.20
0.15
0.10
0.05
0.00
0.0 0.1 0.2 0.3 0.4 0.5 0.6 0.7 0.8 0.9 1.0 1.1 1.2 1.3 1.4 1.5 1.6 1.7 1.8 1.9 2.0
RATIO BINS(MEAS. DEN/MODEL DEN)

Number A19

IDB DATA
KP LIMITS 5.0- 9.0
ALTLIM 0.- 200.
LAT LIM 15.- 30.
NORTHERN HEMISPHERE
MAX Y VAL 66.00
MEAN VALUE 1.04
ST. DEV. 1.13E-01
TOTAL POINTS= 192

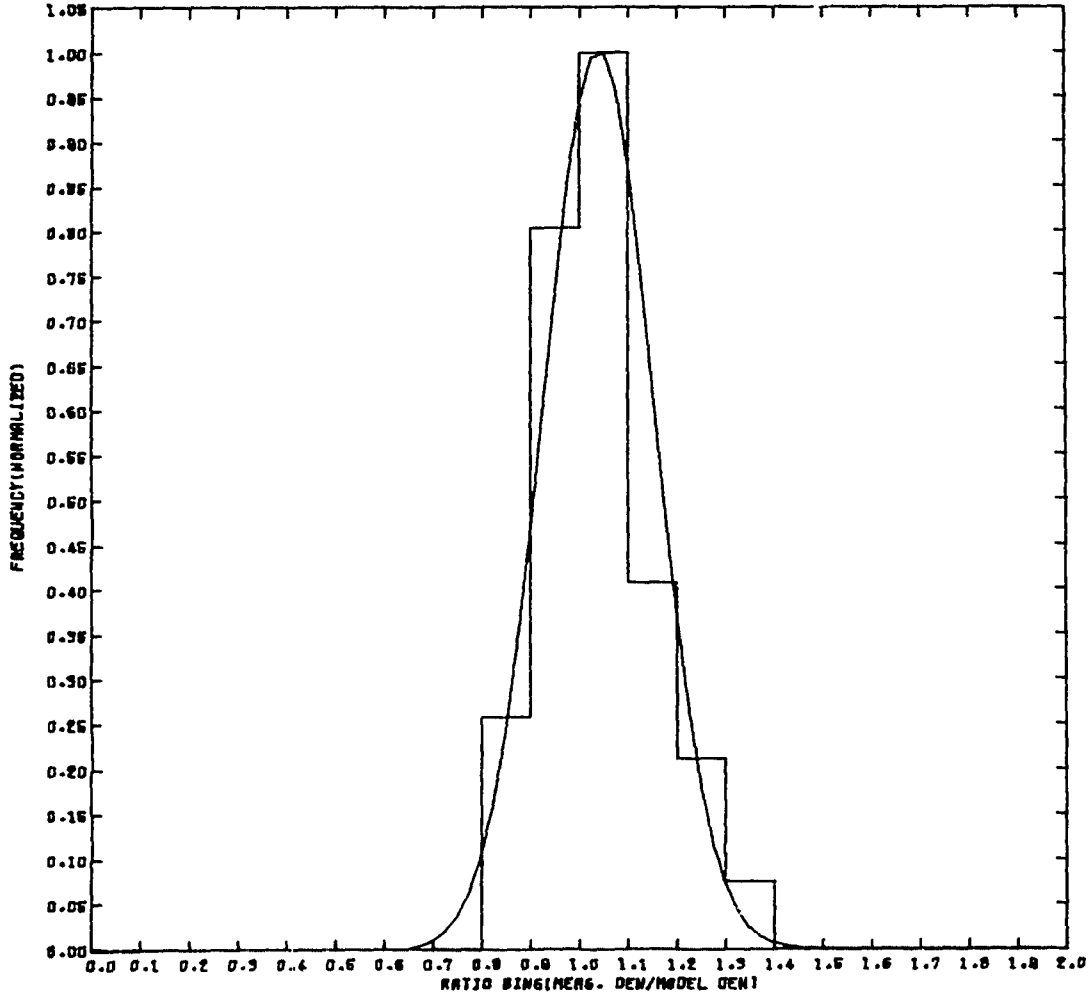

Number A20

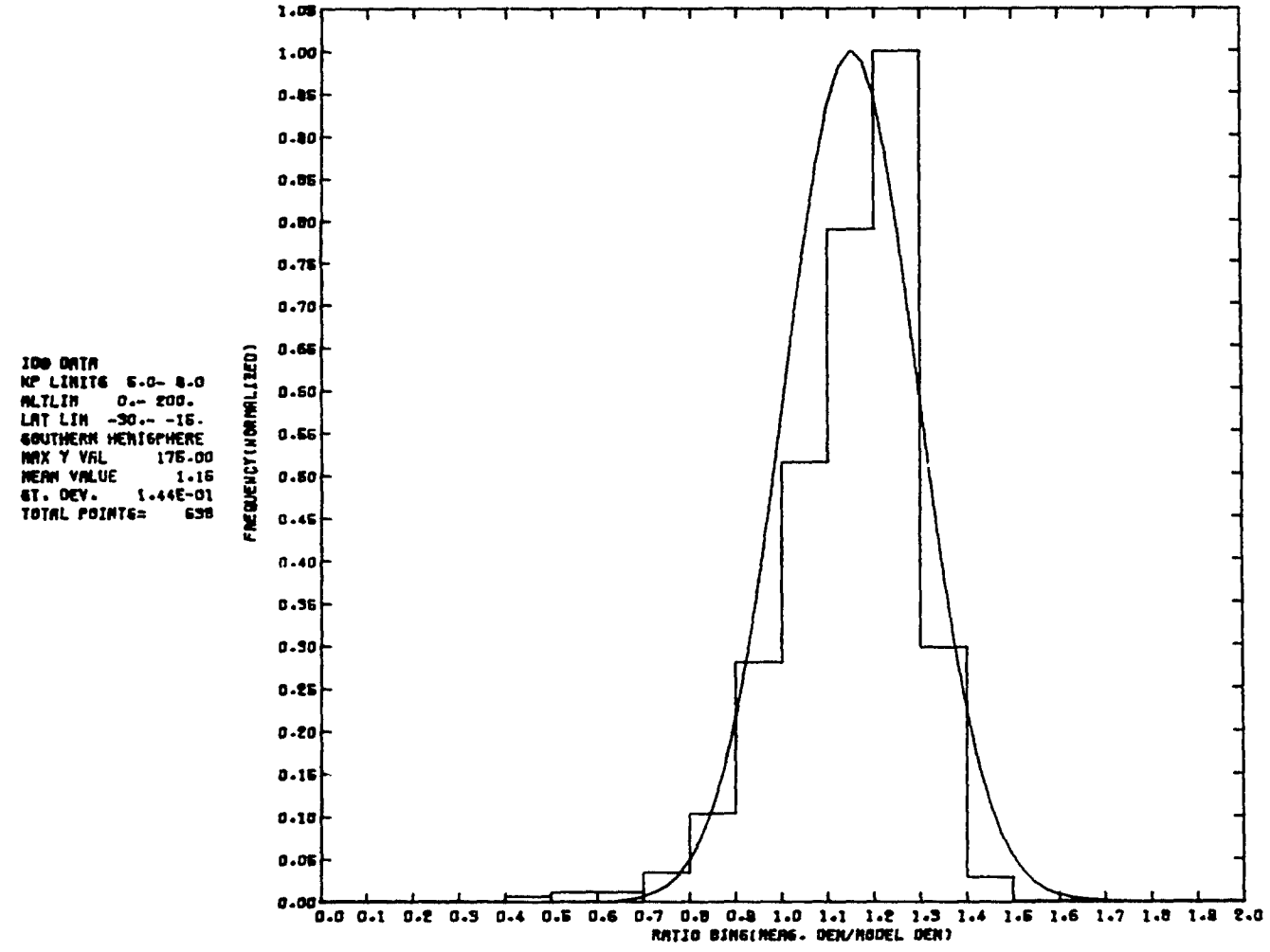
IDB DATA
KP LIMITS 5.0- 8.0
ALTLIM 0.- 200.
LAT LIM -30.- -15.
SOUTHERN HEMISPHERE
MAX Y VAL 175.00
MEAN VALUE 1.16
ST. DEV. 1.44E-01
TOTAL POINTS= 638
FREQUENCY(NORMALIZED)
RATIO BINS(MEAS. DEN/MODEL DEN)

Number A21

IDD DATA
KP LIMITS 3.0- 5.0
ALTLIM 0.- 200.
LAT LIM 30.- 45.
NORTHERN HEMISPHERE
MAX Y VAL 863.00
MEAN VALUE 1.12
ST. DEV. 1.78E-01
TOTAL POINTS= 3159

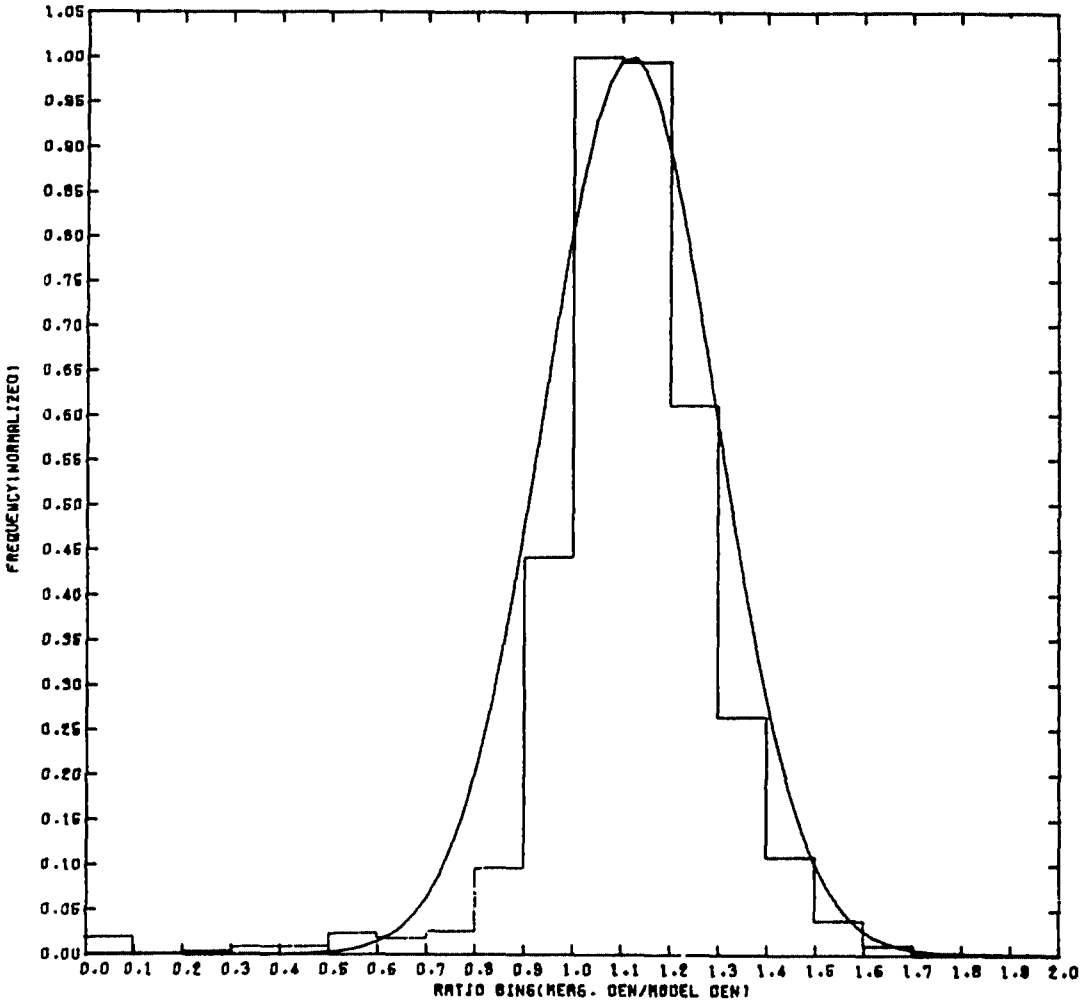

Number A22

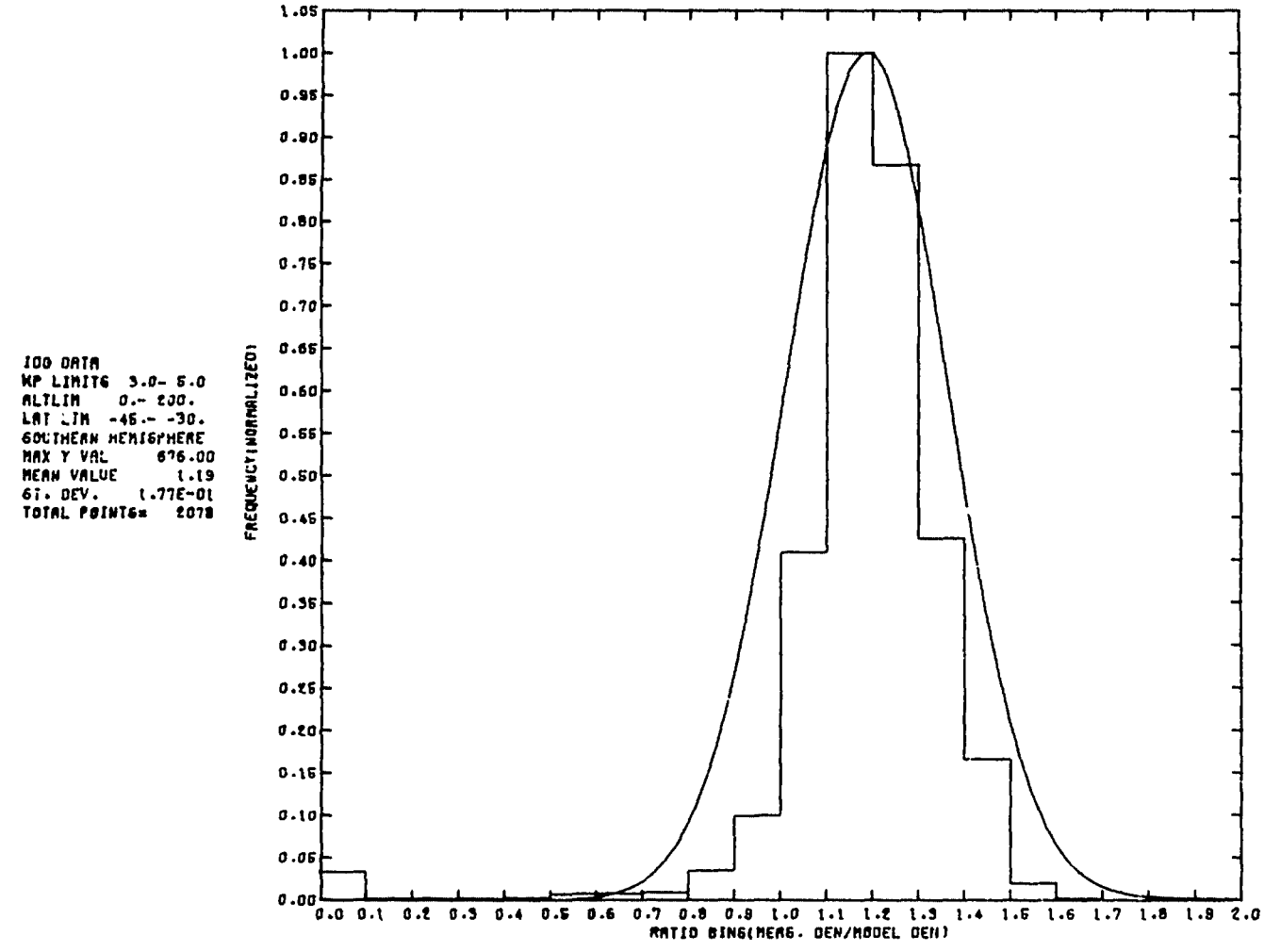
IDD DATA
KP LIMITS 3.0- 5.0
ALTLIM 0.- 200.
LAT LIM -45.- -30.
SOUTHERN HEMISPHERE
MAX Y VAL 676.00
MEAN VALUE 1.19
ST. DEV. 1.77E-01
TOTAL POINTS= 2078
FREQUENCY(NORMALIZED)
RATIO BINS(MEAS. DEN/MODEL DEN)

Number A23

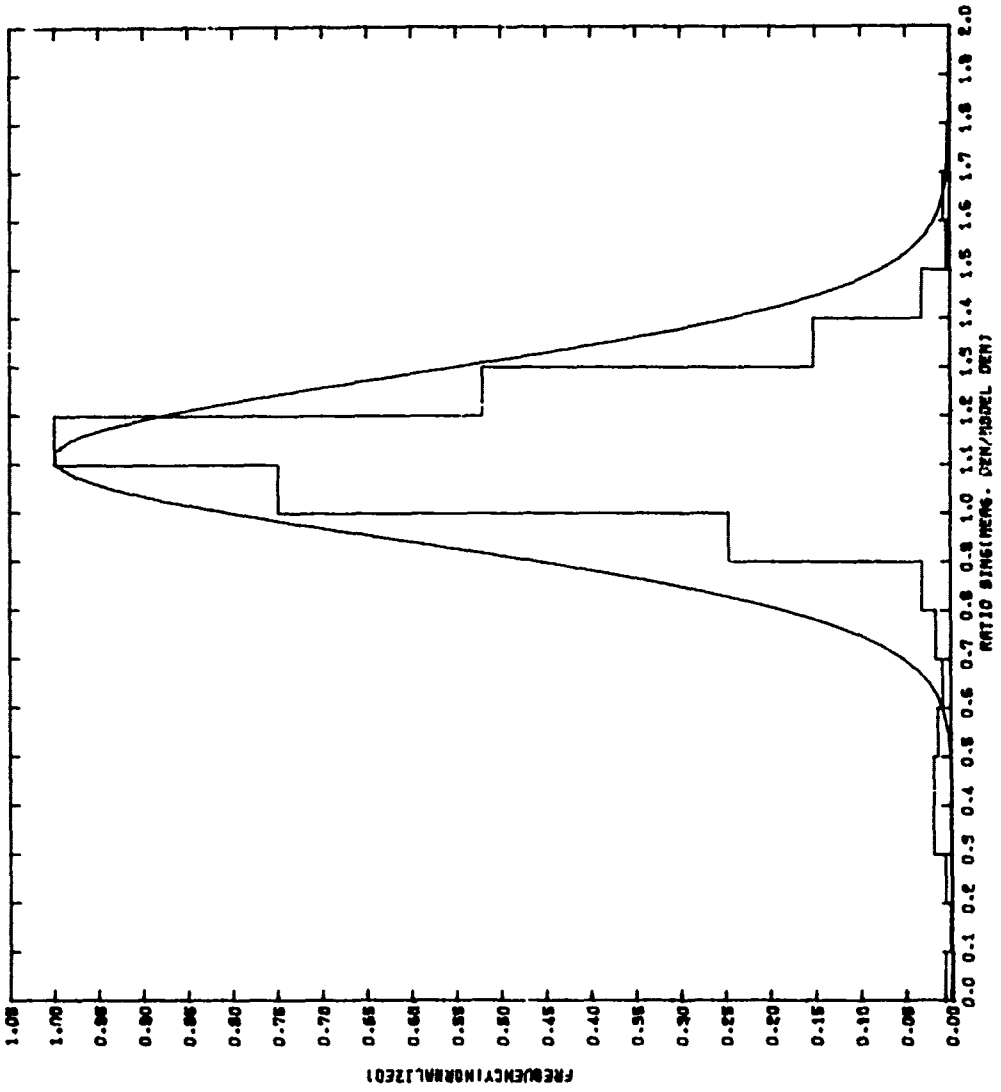
FREQUENCY(NORMALIZED)
RATIO BIN(MEAS. DEN/MODEL DEN)
IGD DATA
KP LIMITS 0.0- 3.0
ALTLIM 0.-- 200.
LAT LIM 60.-- 75.
NORTHERN HEMISPHERE
MAX Y VAL 2760.00
MEAN VALUE 1.11
ST. DEV. 1.71E-01
TOTAL POINTS= 7850

Number A24

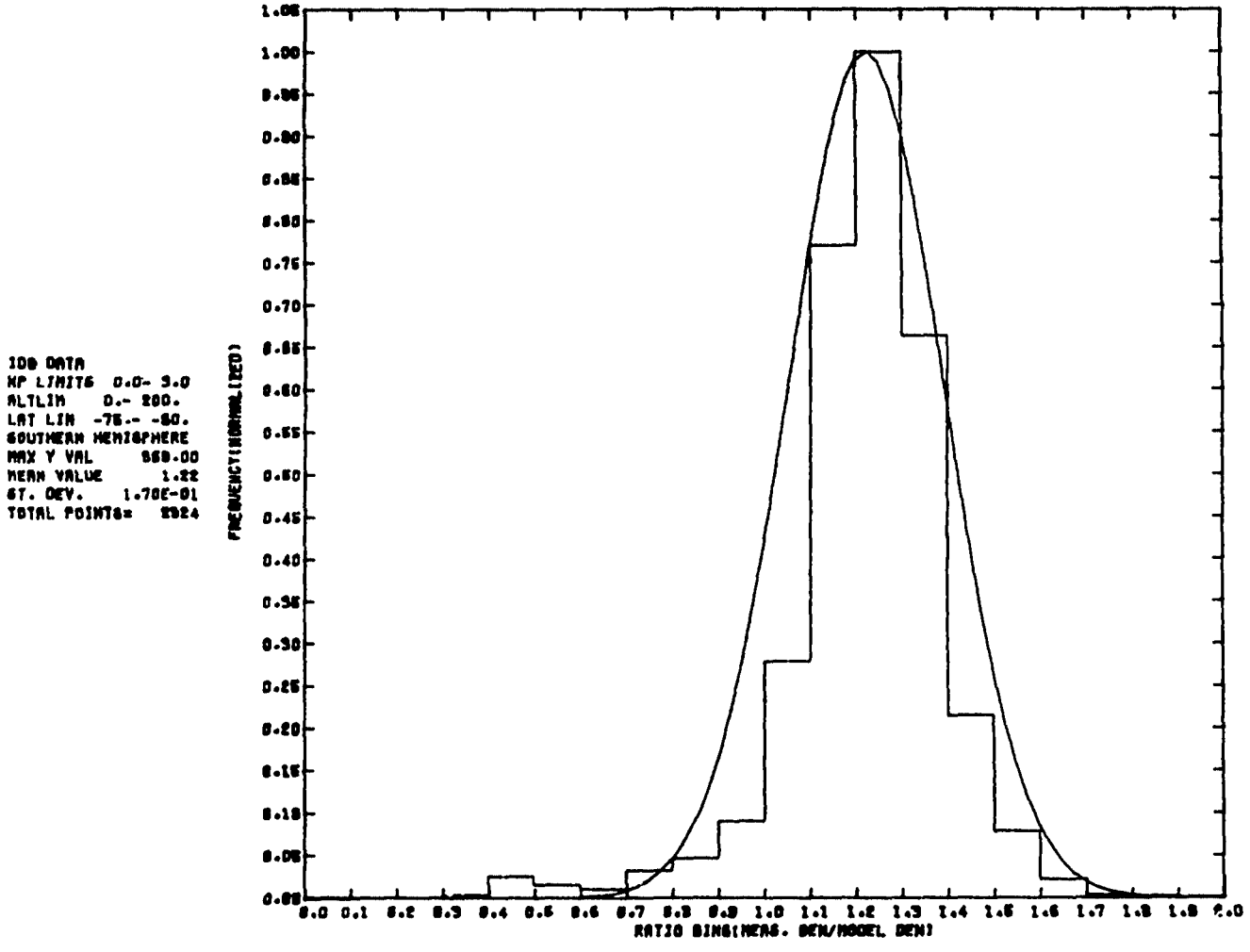
IDB DATA
KP LIMITS 0.0- 3.0
ALTLIM 0.- 200.
LAT LIM -75.- -80.
SOUTHERN HEMISPHERE
MAX Y VAL 559.00
MEAN VALUE 1.22
ST. DEV. 1.78E-01
TOTAL POINTS= 2924
FREQUENCY(NORMALIZED)
RATIO BINS(MEAS. DEN/MODEL DEN)

Number A25

IDO DATA
KP LIMITS 3.0- 5.0
ALTLIM 0.- 200.
LAT LIM -90.- -75.
SOUTHERN HEMISPHERE
MAX Y VAL 158.00
MEAN VALUE 1.34
ST. DEV. 1.78E-01
TOTAL POINTS= 729

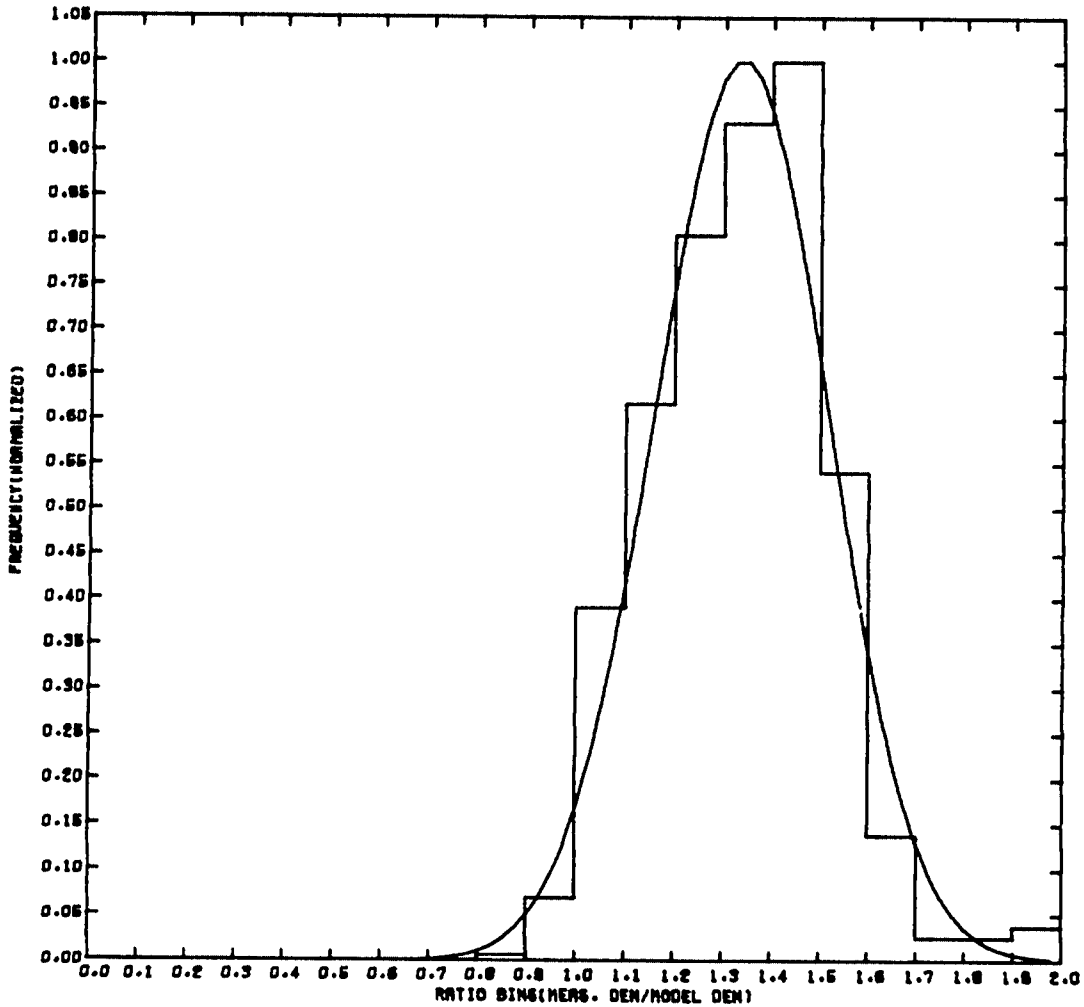

Number A26

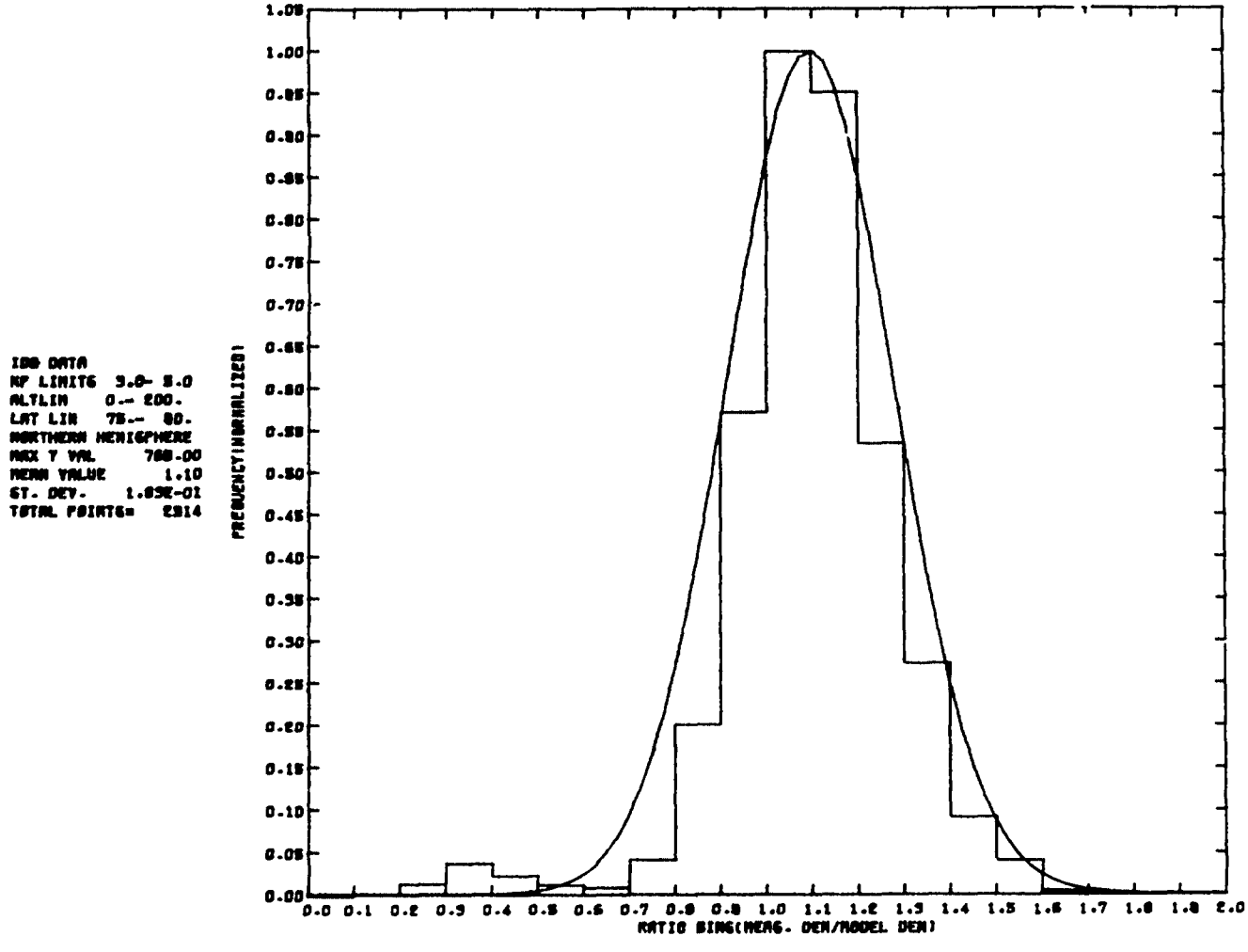
IBB DATA
MF LIMITS 3.0- 8.0
ALTLIM 0.- 200.
LAT LIM 75.- 80.
NORTHERN HEMISPHERE
MAX Y VAL 788.00
MEAN VALUE 1.10
ST. DEV. 1.89E-01
TOTAL POINTS= 2814
FREQUENCY(NORMALIZED)
RATIO BIN(MEAS. DEN/MODEL DEN)

Number A27